(14)

AD______________

PHYSICAL AND CHEMICAL CHARACTERIZATION OF MILITARY SMOKES

Part III-White Phosphorus-Felt Smokes
Final Report

By

Sidney Katz
Alan Snelson
Ronald Butler
Warren Bock
Narayanan Rajendran
Suresh Relwani

29 May 1981

Supported by

US Army Medical Research and Development Command
Fort Detrick, Frederick, Maryland 21701

Contract No. DAMD17-78-C-8085

IIT Research Institute
10 West 35th Street
Chicago, Illinois 60616

Contract Officer's Technical Representative: J.J. Barkley, Jr.
US Army Medical Bioengineering Research and Development Laboratory
Fort Detrick, Frederick, Maryland 21701

Approved for public release; distribution unlimited.

The findings in this report are not to be construed as an official Department of the Army position unless so designated by other authorized documents.

AD______________

PHYSICAL AND CHEMICAL CHARACTERIZATION OF MILITARY SMOKES

Part III-White Phosphorus-Felt Smokes

Final Report

By

Sidney Katz
Alan Snelson
Ronald Butler
Warren Bock
Narayanan Rajendran
Suresh Relwani

29 May 1981

Supported by

US Army Medical Research and Development Command
Fort Detrick, Frederick, Maryland 21701

Contract No. DAMD17-78-C-8085

IIT Research Institute
10 West 35th Street
Chicago, Illinois 60616

Contract Officer's Technical Representative: J.J. Barkley, Jr.
US Army Medical Bioengineering Research and Development Laboratory
Fort Detrick, Frederick, Maryland 21701

Approved for public release; distribution unlimited.

REPORT DOCUMENTATION PAGE	READ INSTRUCTIONS BEFORE COMPLETING FORM
1. REPORT NUMBER 2. GOVT ACCESSION NO. AD-A115 657	3. RECIPIENT'S CATALOG NUMBER
4. TITLE (and Subtitle) Physical and Chemical Characterization of Military Smokes. Part III: White Phosphorus-Felt Smokes.	5. TYPE OF REPORT & PERIOD COVERED Part III--Final Report February, 1980-June 1981 6. PERFORMING ORG. REPORT NUMBER
7. AUTHOR(s) Sidney Katz, Ph.D., Alan Snelson, Ph.D., Narayanan Rajendran, Ph.D., Ronald Butler, Warren Bock, and Suresh Relwani	8. CONTRACT OR GRANT NUMBER(s) DAMD17-78-C-8085
9. PERFORMING ORGANIZATION NAME AND ADDRESS IIT Research Institute 10 West 35th Street Chicago, Illinois 60616	10. PROGRAM ELEMENT, PROJECT, TASK AREA & WORK UNIT NUMBERS 62777A. 3E162777 A846.00.020
11. CONTROLLING OFFICE NAME AND ADDRESS U.S. Army Medical Research and Development Command. Ft. Detrick, Frederick, MD. 21701	12. REPORT DATE 29 May 1981 13. NUMBER OF PAGES 78
14. MONITORING AGENCY NAME & ADDRESS(if different from Controlling Office) U.S. Army Medical Bioengineering Research and Development Laboratory Fort Detrick, Frederick, Maryland 21701	15. SECURITY CLASS. (of this report) Unclassified 15a. DECLASSIFICATION/DOWNGRADING SCHEDULE

16. DISTRIBUTION STATEMENT (of this Report)

Approved for public release; distribution unlimited

17. DISTRIBUTION STATEMENT (of the abstract entered in Block 20, if different from Report)

18. SUPPLEMENTARY NOTES

19. KEY WORDS (Continue on reverse side if necessary and identify by block number)

Smoke
Screening smoke
Obscuring smoke
Smoke generation
Phosphorus smoke
White phosphorus-felt smoke
phosphoric acid smokes

20. ABSTRACT (Continue on reverse side if necessary and identify by block number)

An investigation of the U.S. Army White phosphorus-felt smoke munition is described in this report. The study included the chemical characterization of the smoke-generating materials, the physical and chemical analysis of the smoke, and observations of the fog stability. The wedge-shaped generating munition is a pellet consisting of about 80% by weight of phosphorus somewhat irregularly distributed in the felt matrix. Principal impurities in the phosphorus were boron, silicon, iron, and arsenic, all at concentration levels near 0.1 to 0.01%. No significant levels of metallic impurities were present in the felt.

DD FORM 1 JAN 73 1473 EDITION OF 1 NOV 65 IS OBSOLETE

Chemical analysis of the smokes indicated that they were predominantly polyphosphoric acids. Identification was made of the first eight members of the series beginning with orthophosphoric acid and continuing to octaphosphoric acid. Higher members of the series were detected, but were not separated. Small traces of hydrocarbon and nitrogen derivatives were detected at the parts per million level and lower. No organophosphorus compounds were detected. Particle size distributions tended to center around 1.0 μm within a very narrow size distribution. Aging a cloud over a two-hour period led to slight increases in particle size.

☒
☐
☐

...odes
.../or
Di: ...ial

A

EXECUTIVE SUMMARY

This report describes an investigation of phosphorus smokes formed in the combustion reaction of white phosphorus impregnated in a felt substrate. This munition is listed as a developmental item in the present military inventory. The field operation consists of the deployment of an assembly of 128 wedge-shaped units in the target area, with combustion and smoke generation following spontaneously on exposure to the atmosphere.

Each wedge-shaped unit is a 90° sector of a disc, 5 in. in diameter and 0.625 in thick.

A chemical analysis of a representative sample of the material indicated a non-uniform distribution of phosphorus, comprising about 80% of the wedge's weight . Major impurities in the phosphorus were boron (0.0715%), silicon (0.0377%), iron (0.0094%), and arsenic (0.0084%). No significant metal impurities were detected in the felt.

The major chemical constituents of the smoke generated by the burning munition were a series of polyphosphoric acids, orthophosphoric acid (H_3PO_4), pyrophosphoric acid ($H_4P_2O_7$) and higher members, of which members of the series up to polymer number 8 were identified. The first three acids were about 35% of the total, the next five, 27%, with the remaining 38% unresolved higher acids. No other phosphorus acids were observed. Free phosphorus vapor as well as hydrogen and carbon monoxide were detected at the parts per million level and, at much lower concentrations, methane, ethylene, carbonyl sulfide (COS), acetylene, hydrogen cyanide, dicyanobenzenes, acetonitrile and acrylonitrile. No organophosphorus compounds were observed.

The particle size distributions of the smokes centered at near 1.0μm with a very narrow size distribution. Humidity appeared to have little effect on size distribution, and aging over two-hour intervals also produced minor size increases.

FOREWORD

This report on the physical and chemical characterization of the white phosphorus-felt smoke generating munition and the generated smoke is the third in a series of investigations of military screening smokes. The study was begun on February 1, 1980 and the experimental work was concluded on March 31, 1981.

Prior studies in the series included similar characterization of hexachloroethane smokes, completed on May 31, 1979 and oil fogs generated from Type SGF-2 fog oils, completed on February 28, 1980. These studies are all phases of a program titled *Physical and Chemical Characterization of Military Smokes*, U.S. Army Contract No. DAMD11-17-78-C-8085.

Citation of trade names in this report does not constitute a Department of the Army endorsement or approval of the use of such items.

The close cooperation of Mr. Jesse J. Barkley, Jr., of the U.S. Army Medical Bioengineering Research and Development Laboratory is gratefully acknowledged.

CONTENTS

LIST OF FIGURES

LIST OF TABLES

SYMBOLS AND ABBREVIATIONS

ASAS	Active scattering aerosol sensor (instrument)
b	constant term in regression equation
C	degrees celsius
C_i	aerosol mass concentration in stage i (Piezoelectric counter)
cm	centimeters
cm^3, cc	cubic centimeters
conc	concentration
d_i	midrange diameter
$\bar{d}_m$	mass mean aerodynamic diameter
$\bar{d}_n$	mass mean diameter
EDTA	ethylene diamine tetraacetic acid
g	grams
GC	gas chromatograph
HPLC	high pressure liquid chromatograph
ID	inside diameter
l	liter
m	meter
m	slope in regression equation
m^3	cubic meter
M_i	midpoint diameters between stages (Piezoelectric counter)
min	minute
ml	milliliter
mm	millimeter
MMD	mass median diameter
MS	mass spectrometer
NMD	number median diameter
OD	outside diameter
ppb	parts per billion
ppm	parts per million
P/Z	Piezolectric Particle Counter
R	correlation coefficient (assuming log normal distribution)

R_f	retention factor (chromatography)
RH	relative humidity
SGF-2	U.S. Army smoke generating fuel designation
SL	significance level
soln	solution
t	time
TIC	total ion current (mass spectrometry)
TLC	thin layer chromatography
TSP	total suspended particles
v	volume
V	volume flow rate
w, wt	weight
X_i	mass fraction in stage i
Δf_i	frequency shift for stage i
Δt	sample time
J_i	sensitivity factor for stage i
ρ	particle density
σ_g	geometric standard deviation
σ_i	sensitivity factor for stage i (piezoelectric particle counter)

1. INTRODUCTION

This investigation is the third in a series of studies on military obscuration smokes which are presently in the inventory or under advanced development by the U.S. Army. These investigations have included examinations of the smoke-generating materials, the generating process and the physical and chemical properties of the product smokes with emphasis on physiological consequences of exposure. The study of the physical properties of the smokes was limited to the particle size ranges below 10 μm where pulmonary retention is predominant.

Part 1 of this series, dated January 1, 1980, was a report on smokes produced by the Army HC smoke generator in a process involving the generation of zinc chloride smokes by the thermochemical interaction of hexachloroethane, zinc oxide and aluminum.

Part 2, dated June 1, 1980, described both the oils and the oil fogs formed in the thermal evaporation and condensation of SGF-2 fog oils. These oils are a middle distillate group of hydrocarbon oils, somewhat heavier than gasolines and diesel oils. In the field, fog generation employs a gasoline powered M3-A3 fog generator.

The present report describes an investigation of phosphorus smokes formed by the combustion in air of white phosphorus impregnated in felt substrates.

The white phosphorus-felt munition is presently listed as developmental. It consists of an assembly of wedge-shaped elements, each of which is a felted substrate impregnated with elemental white phosphorus. When the assembly is deployed, a central burster charge separates the wedges. Contact with atmospheric oxygen and the heat of the deployment process combine to initiate the smoke generating reactions.

Physical characterization of the fog involved its generation in chambers at various humidities followed by sampling to determine the number concentrations and size distributions of the smoke particles. Chemical studies were made to identify impurities in the phosphorus, the composition of the felt materials and the reaction products of the felt-phosphorus reaction. A problem of major concern was the identification of potentially hazardous products of the pyrolytic reactions of the organic felt-phosphorus materials.

2. CONCLUSIONS

White phosphorus-felt wedges were examined physically. It was evident that the phosphorus distribution was very irregular, with a median value of about 80% of the total mass. Principal impurities in the phosphorus were boron (0.07%), silicon (0.04%), iron (0.008%), and arsenic (0.008%). No significant metal impurities were present in the felt.

Smoke generated by burning samples of the wedge material was collected and examined for phosphorus derivatives. Fairly large variations in the analytical results are attributed to the variations in the compositions of the wedge materials.

The identified acid components of the munition smoke were polyphosphoric acids ranging in polymer numbers from 1 to 8. Ortho-, pyro-, and triphosphoric acids were about 35% of the total with the tetra- to octaphosphoric members totalling about 27%. The remaining 38% consisted of higher phosphoric acids which were not resolved by the separation process. Other phosphorus acids including phosphinic, phosphorous and metaphosphoric acid were not detected. As the smokes aged over several days, the higher polymers of the series depolymerized to form the lower members.

A number of organic compounds and several permanent gases were identified in the smoke. The most abundant, hydrogen, carbon mononxide, and phosphorus were present in the smoke at levels of 1 to 10 ppm by volume. Other materials present at parts per billion (ppb) levels included methane, ethylene, carbonyl sulfide (COS), acetylene, hydrogen cyanide, 1,4-dicyanobenzene, 1,3-dicyanobenzene, 1-2 dicyanobenzene, acetonitrile ($HO \cdot CH_2CN$) and acrylonitrile ($CH_2:CHCN$).

These materials and many other compounds with related structures were detected in concentrations below the ppb level and also below their TLV.*

---

*Threshold Limit Values for Chemical Substances and Physical Agents in the Workroom Enviroment. American Conference of Governmental Industrial Hygienists, Cincinnati, Ohio 1979.

Smoke particle size distributions were measured at humidities between 5% and 75%. The particle diameters center around 1.0 μm with a very narrow distribution range, with 98% of the particles below 2 μm. Humidity has slight effect on the size distribution. With aging over a two hour interval, the median size increased slightly from about 1.1 to 1.3 μm.

3. WHITE PHOSPHORUS SMOKE GENERATION

3.1 FIELD GENERATION

The white phosphorus-felt munition is a cylindrical assembly, 21.75 inches long and 5.0 inches in diameter. The assembly consists of 32 disc-shaped members, 5/8 inches thick, mounted on an axial support tube of 1 1/8 inches diameter. Each disc consists of four wedge-shaped elements which are the actual white phosphorus-felt smoke generators. In a field operation, the assembly is propelled into the area and activated, releasing and scattering the 128 wedges. The wedges ignite in the atmosphere to generate the product smoke.

3.2 LABORATORY SMOKE GENERATION

The smoke generating munition reacts spontaneously in the atmosphere. In the present study, the two operations of chemical characterization and physical assessment were conducted as separate tasks. Smoke generators were constructed for each of these tasks. They are described separately in the following sections.

4. CHEMICAL STUDIES

4.1 INTRODUCTION

The chemical analysis of the white phosphorus munitions was addressed in four phases:

- a procedure for burning the munition in a controlled environment
- a smoke sampling system
- a qualitative analysis to determine the composition of the smoke
- based on the above three phases, a procedure was designed to collect and to analyze quantitatively the chemical species identified in the qualitative study

The overall analytical procedure is summarized in the flow chart in Figure 1. Details are described in the following sections.

4.2 PRELIMINARY ANALYSIS

Smoldering Felt Smoke

As a preliminary to determining the organic species in the munition smoke, an experiment was performed in which the phosphorus-free munition felt material was heated to smoldering and the resulting smoke was collected and analyzed.

To produce the smoke, a piece of felt material approximately one cubic inch in volume was placed on a steel plate heated with a Fischer burner. The resulting smoke was then aspirated through an inverted glass funnel and was collected by bubbling through about 350 ml of methanol. The felt was smoldered to ash in about 30 minutes after which all glass surfaces were washed free of residue with methanol. Wash solutions were combined with the collection solution and were reduced in volume to about 2 ml by evaporation with dry N_2. Prior to analysis the resulting solution was filtered using a Millipore Corporation filter with a 0.2 µm pore size. Analysis was accomplished by capillary gas chromatography using the conditions listed in Table 1. During some experiments the procedure was altered slightly by igniting the smoke with an oxygen/methane torch prior to collection.

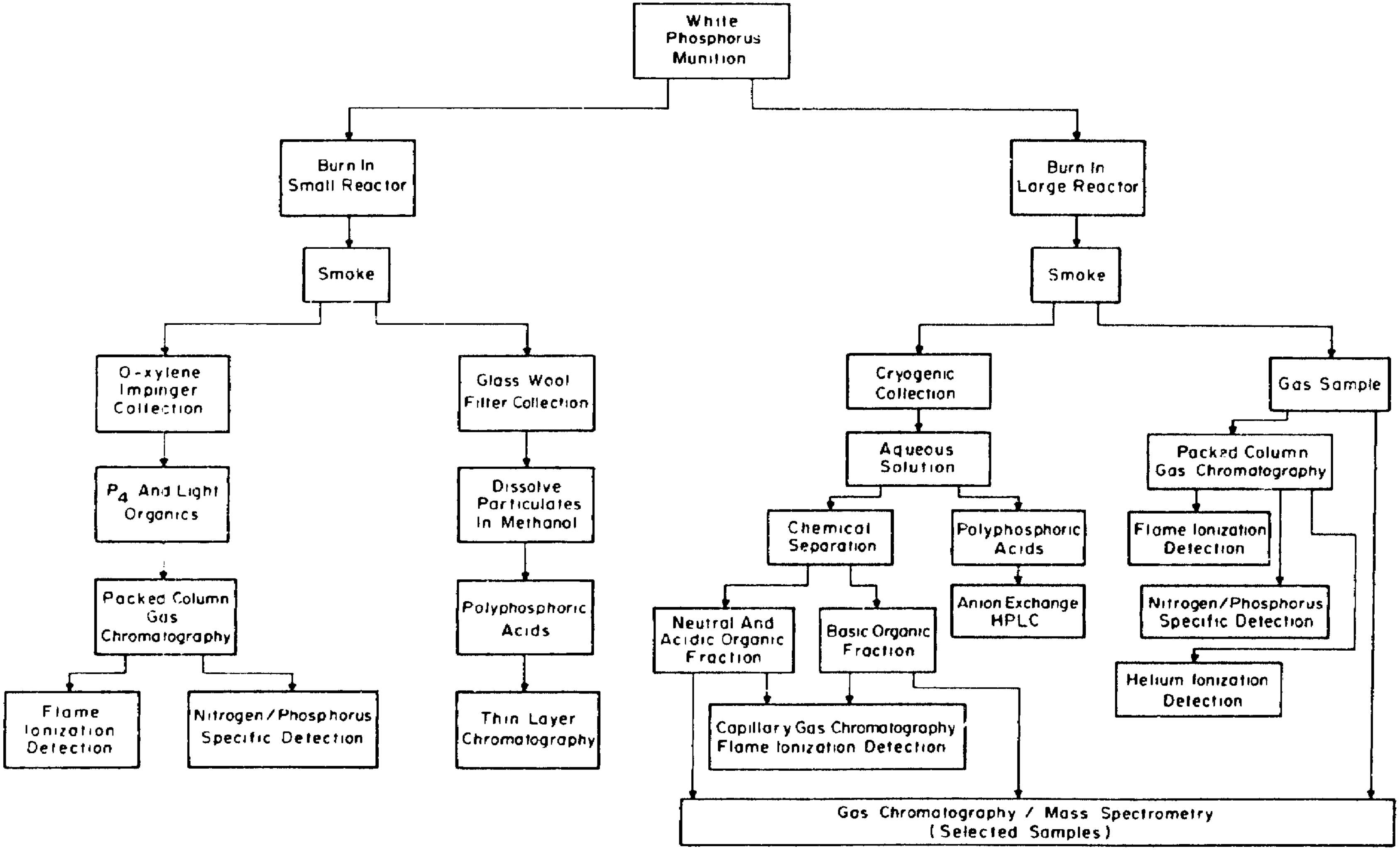

Figure 1. FLOW CHART OF CHEMICAL ANALYSIS OF WHITE PHOSPHORUS MUNITION

TABLE 1. ANALYTICAL PROCEDURE FOR ORGANIC ANALYSIS (FELT SMOKE, MUNITION SMOKE)

Chromatograph:	Hewlett-Packard Model 5840A high resolution gas chromatograph
Column:	25 meter x 0.2 mm ID fused quartz capillary column
Detector:	Flame ionization
Carrier Flow:	∿1.0 ml/min (He)
Purge Flow:	40 ml/min (He)
Make-Up Flow:	30 ml/min
Injector Temp:	180°C
Detector Temp:	275°C
Oven Temp:	40°C for 7 min, program at 3°C/min to 210°C and hold for 20 min
Purge Initiation:	1 min after injection

Small Reactor System

Smoke for preliminary analysis was generated in a small glass reactor capable of burning phosphorus munition in a controlled environment (constant humidity and constant air flow rate).

Constructed of glass with glass and teflon valves, the system consisted of two air flow controllers and meters (Matheson rotameter), two H_2O saturating bubblers, a one-liter glass air mixing chamber, the reactor itself, and various collection apparatus. The reactor was a glass cylinder 2.5 cm in diameter and 6 cm long. It was provided with a perforated ceramic burning surface, a nitrogen inlet, four symmetrically placed air inlets and a large diameter smoke exit. A schematic of the system is shown in Figure 2 and a photograph of the reactor is shown in Figure 3.

During a typical experiment a small piece of munition (about 0.2 g) was cut from stock munition, dried and weighed under nitrogen and placed in the nitrogen purged reactor. Humidity and air flow rate were selected via the flow controllers, and the valves were switched to allow air to flow into the reactor. Smoke was produced spontaneously and then passed through the collection devices.

Two types of collectors were used with the small reactor. For particulate collection a 3 cm length of 6 mm OD glass tubing packed with glass wool placed at the reactor exit served as an effective collection filter. For collection of P_4 and light organics, three o-xylene impingers were placed in series at the reactor exit. Each impinger contained approximately 10 ml of oxygen-free o-xylene.

Thin Layer Chromatography of Polyphosphoric Acids

Thin layer chromatography (TLC) was selected as an analytical method for screening the phosphoric acid species in the munition smoke.

Several solvent systems and visualization techniques were tested on model compounds. Finally, a two dimensional TLC approach was selected using the following two solvent systems:

Solvent System S0:	conc. NH_3 soln./methanol/isobutyl alcohol/water (9:50:10:31)
Solvent System S2:	isopropyl alcohol/water/20% trichloroacetic acid soln./conc. NH_3 soln. (70:10:20:0.3)

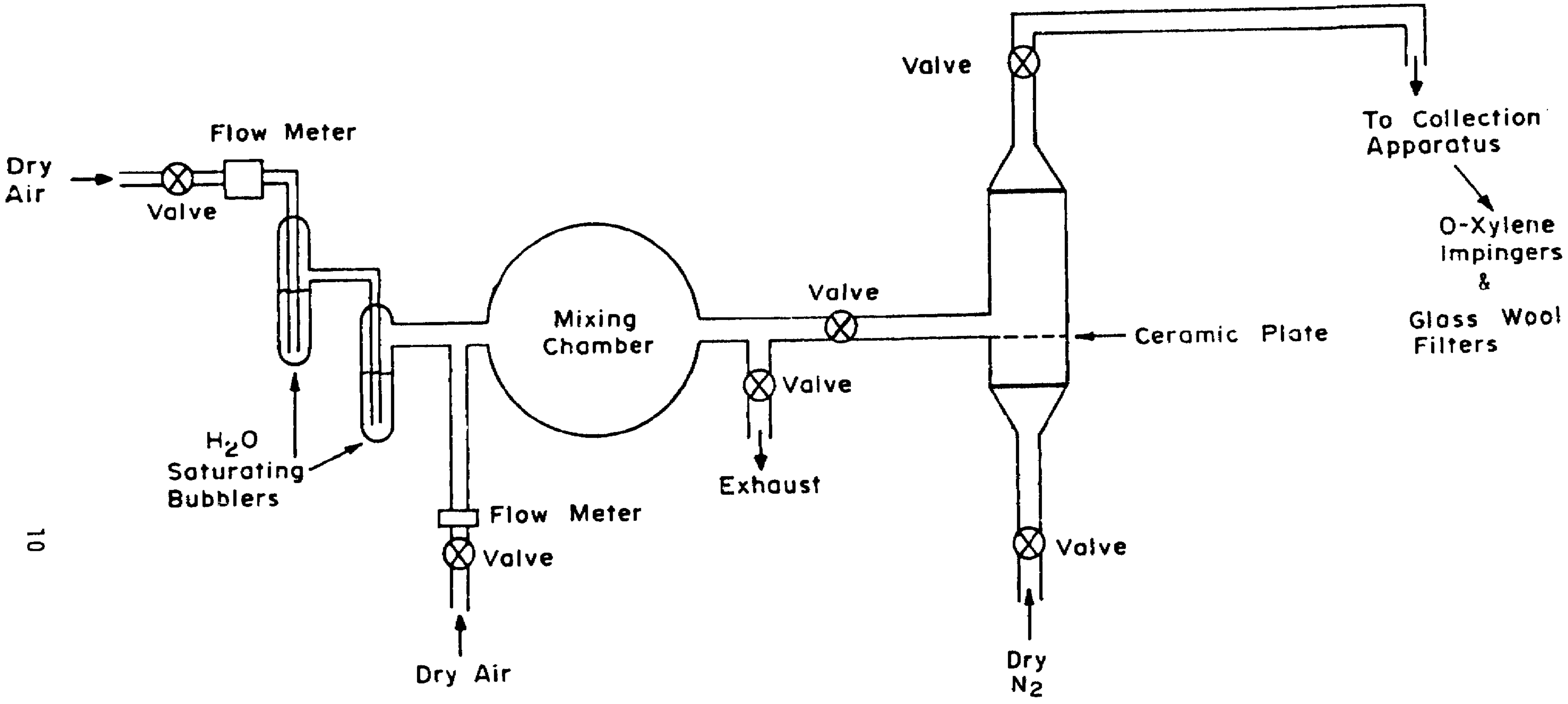

Figure 2. Schematic diagram of small reactor system.

Figure 2. [illegible] reaction system

Visualization of spots was accomplished using a Haynes-Isherwood ammonium molybdate solution prepared as follows: 1 g of ammonium molybdate was dissolved in 40 ml of H_2O followed by 3 ml of concentrated HCl, 5 ml of concentrated $HClO_4$ and diluted to a final volume of 100 ml with acetone. After spraying the developed microcrystalline cellulose TLC plate with reagent, exposure to ultraviolet light was necessary to fully visualize the spots.

After completion of the burning phase of an experiment, the glass wool filter was removed and the acid species was dissolved in 3 ml of methanol. The TLC plate was then spotted with a 1 to 10 µl spot and developed. Species identification was accomplished using a combination of retention factor (Rf) values and spot colors.

To standardize the plates initially, the following phosphorus acids were obtained from Tridom/Fluka; phosphinic acid (H_3PO_2), phosphorous acid (H_3PO_3), phosphoric acid (H_3PO_4), meta-phosphoric acid $(HPO_3)n$, pyrophosphoric acid ($H_4P_2O_7$), and polyphosphoric acid ($\approx 60\%\ H_5P_3O_{10} + \approx 15\%\ H_4P_2O_7 + \approx 10\%\ (HPO_3) + 15\%\ (HPO_3)x$.

O-xylene Impinger Analysis For P_4

Upon completion of the phosphorus munition burning phase, the impingers were removed from the system and 25 µl of 1-nitropropane internal standard (283 µmoles) was added to each. Approximately 0.5 ml of each sample was then pipetted into a gas chromatograph autosampler vial and analyzed in triplicate using the conditions summarized in Table 2.

Phosphorus calibration standards were prepared weekly from stock reagents. Each standard contained from 10 to 50 µmoles P_4 and 25 µl of 1-nitropropane per 100 ml of o-xylene solvent. Calibrations were performed daily in triplicate and were constantly cross checked with older standards to determine stability and linearity. Generally, calibration standards were useful for only 1 to 3 weeks after which they were discarded.

4.3 FINAL ANALYSIS

Large Reactor System

Experience gained with the small reactor system suggested the need for two experimental changes. First, to average the effects of inhomogeneous areas in

TABLE 2. ANALYTICAL PROCEDURES FOR P_4 ANALYSIS

Chromatograph:	Hewlett-Packard Model 5840A Gas Chromatograph
Column:	3 ft x 2 mm I.D. glass column packed with Porapak N, 100/120 mesh
Detector:	Nitrogen/phosphorus specific
Carrier Flow:	25 ml/min helium
Injector Temp:	180°C
Detector Temp:	275°C
Oven Temp:	75°C for 5 min, up at 5°C/min to 200°C and hold for 40 min

the munition, it was decided to burn larger pieces of material. Second, it was believed that a method of trapping 100% of the smoke followed by later sample preparation and analysis would be superior to the previous system of impingers and filters.

The first change was effected by building a reactor capable of burning munition pieces weighing up to 20 g. The new reactor consisted of a glass cylinder 6 inches in diameter and 2 ft long. Air or nitrogen was introduced through four stainless steel inlets at the base of the reactor and products exited through a 1 inch I.D. glass and kovar tube attached to the side of the reactor. A 2 inch diameter stainless steel platform set in the base of the reactor provided a burning surface. The air inlet system was modified by replacing the two H_2O bubblers with a series of four higher capacity bubblers.

The new product trapping system was constructed by placing three 2-in. OD liquid oxygen cooled cold traps in series at the reactor exit. A one liter evacuated flask attached at the reactor exit via a tee joint just prior to the cold traps served as a gas sampler. A photograph of the reactor and cold traps is shown in Figure 4.

Burning and Separation Procedure

With the exception of the larger samples, the burning procedure was the same as that described for the small reaction. Some collector manipulation was required as the traps had to be continually topped with liquid oxygen, the connecting lines had to be periodically tapped to break up deposits of solid condensates, and a valve had to be cracked open to bleed gas into the evacuated flask.

After burning was complete, the munition was removed and weighed to determine weight loss and the approximate amount of unburned phosphorus.

The three traps were removed, allowed to warm to ambient temperature and were washed twice each with 75 ml of H_2O followed by two washes each with 75 ml of methylene chloride. The reactor walls were then washed with 500 ml of H_2O and this was combined with the aqueous washes from the traps. One ml of this solution was removed, filtered with an 0.2 μm filter and reserved for HPLC analysis for polyphosphoric acids.

The remaining aqueous solution was extracted twice with equal volumes of methylene chloride, combined with the methylene chloride trap washes, dried

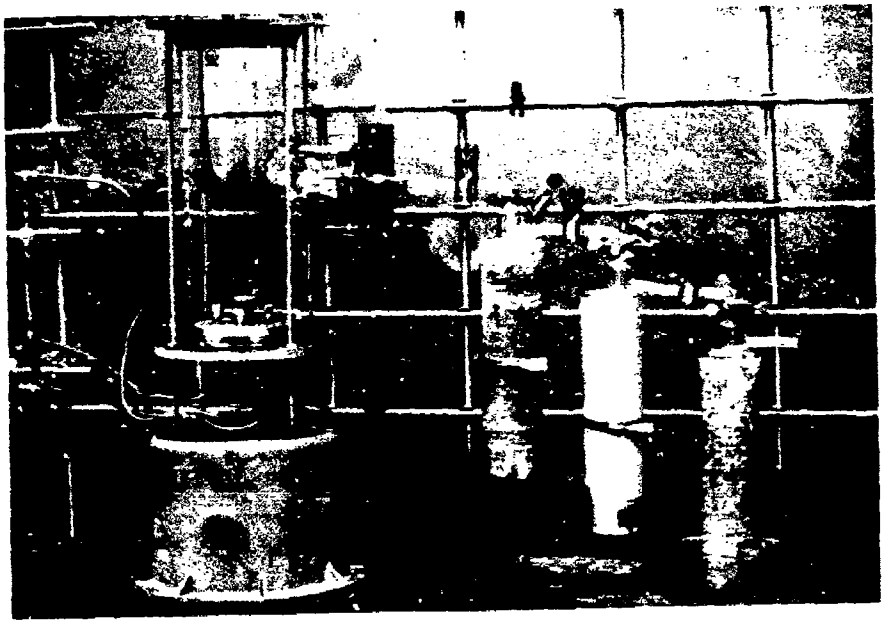

Figure 1. Large reactor system

with sodium sulfate (Na_2SO_4), filtered, rotary evaporated to 10 ml and blown dry with a nitrogen stream. The resulting sample was dissolved in 0.5 ml of methylene chloride containing the internal standard and was analyzed for organics by capillary gas chromatography.

HPLC Polyphosphoric Acid Analysis

Polyphosphoric acids were separated and analyzed by an anion HPLC method suggested by Yamaguchi.[1] In this method, the HPLC is coupled with a commercial automatic phosphate analyzer. Analytical parameters are summarized in Table 3.

The system was calibrated using a standard orthophosphoric acid solution and retention times were determined by the injection of a commercial mixture of polyphosphoric acids (Tridom/Fluka).

Total phosphorus content of the aqueous solution was determined by oxidation to orthophosphoric acid followed by HPLC analysis. Oxidation was achieved by adding 0.5 ml of concentrated nitric acid to an equal volume of sample and heating to 100°C for 15 minutes. HPLC analytical parameters were identical to those previously described except that the analysis was isocratic with Mobile A to B phase ratio of 70:30.

The collected phosphorus acid solution, obtained from burning the phosphorus-felt wedge munition, was subjected to analysis immediately after collection to minimize possible hydrolysis effects on the composition of the acid mixture. Consequently, each collected acid sample could be subjected to only one analytical determination.

Oxidized samples were generally analyzed in duplicate or triplicate. Electronic integration of peak areas was not feasible due to the unusually large peak widths, therefore, it was necessary to measure areas manually with a planimeter.

Gas Sample Analysis

Gas samples were removed from the 1-liter gas sampling flask via a 1 ml precision sampling series A-2 gas syringe and were analyzed by three gas chromatography methods as summarized in Table 4.

Prior to each analysis.the instruments were calibrated using the appropriate standard. Gas standards containing light hydrocarbons, carbon monoxide,

TABLE 3. HPLC ANALYSIS OF POLYPHOSPHORIC ACIDS

Chromatograph:	Waters Associates Model 244 with the following units: Model 6000A Solvent Delivery System (2 units) Model 660 Solvent Programmer
Detector:	Scientific Instruments Corporation Model CFA 200 Autoanalyzer configured for Phosphate Analysis
Column:	Whatman Partisil SAX
Flow Rate:	1.0 ml-min^{-1}
Mobile Phase A:	0.1 M Na_2SO_4 + 5 mM disodium EDTA
Mobile Phase B:	1.0 M Na_2SO_4 + 5 mM disodium EDTA
Gradient:	100% A to 100% B in 2 hours using gradient curve 5
Injection Volume:	25 to 50 µl

TABLE 4. GC ANALYSIS OF GAS SAMPLES

	PH_3 and Light Nitrogen Containing Compounds	Light Hydrocarbons	Permanent Gases
Chromatograph:	Hewlett-Packard 5840A	Packard 427	Varian 2700 Trace Gas Analyzer
Integrator:	Not required (part of 5840A system)	Hewlett-Packard 3390A	Hewlett-Packard 3380A
Column:	3 ft. x 2 mm glass packed with 100/120 mesh Porapak N	6 ft. x 1/8 in. stainless steel packed with 80/100 mesh carbosphere	10 ft. x 1/8 in. stainless steel packed with 80/100 mesh Porapak Q or 20 ft. x 1/8 in. stainless steel packed with 100/120 mesh Molecular Sieve 5A
Detector:	Nitrogen/Phosphorus Specific	Flame Ionization	Helium Ionization
Carrier Flow:	30 $ml\text{-}min^{-1}$ Helium	30 $ml\text{-}min^{-1}$ Helium	30 $ml\text{-}min^{-1}$ Helium (both columns)
Injector Temp:	180°C	150°C	Ambient
Detector Temp:	275°C	250°C	250°C
Oven Temp:	75°C for 5 mins., up at 5°C/min. to 200°C and hold for 40 min.	100°C for 1 min. up at 12°C/min. to 350°C and hold for 15 mins.	100°C isothermal (both columns)
Injection Volume:	0.5 ml	0.5 ml	8 ml (via an injection loop at a measured pressure from 10 to 800 torr)

hydrogen, phosphine, hydrogen cyanide and carbonyl sulfide were obtained commercially from the Matheson Company. A standard mixture containing acetonitrile, (CH_3CN), acrylonitrile ($CH_2{:}CH{\cdot}CN$) and propionitrile (C_2H_5CN) in methylene chloride was prepared in the laboratory for the purpose of calibrating for light nitrogen-containing compounds.

All gas analysis was run in duplicate and in triplicate if time permitted.

Organic Analysis

As mentioned previously, organic samples were analyzed by capillary gas chromatography using the conditions summarized in Table 1.

Organic species were identified by GC/MS (described below). Using this information, a standard mixture was prepared for calibration purposes. The composition of the standard is listed in Table 5. All samples were autosampler injected (0.5 μl injection size) and analyzed in triplicate. Calibrations were performed daily, also in triplicate.

Gas Chromatography/Mass Spectrometry

For GC/MS analysis of selected fractions, the following system was used. A Varian Mat 311A mass spectrometer was used featuring a double-focusing analyzer system with Nier-Johnson geometry and a differentially pumped vacuum system utilizing two high-speed turbomolecular pumps. For sample introduction the system used a Varian Aerograph Model 2740 gas chromatograph equipped with a Hewlett-Packard Model 18835A injection system for splitless capillary column analysis. The capillary column was directly interfaced with the mass spectrometer via a microneedle valve regulator and glass lined tube. When using a packed column, the column was interfaced via a glass jet separator system.

The ion source of the mass spectrometer consisted of a combined electron impact/electron impact ionization detector for simultaneous registration of electron impact mass spectra and total ion current (TIC) gas chromatograms. The TIC signal was fed to an electronic integrator to monitor the progress of the chromatogram in real time.

The column and the gas chromatographic parameters were identical to those used earlier in the gas chromatographic analysis. As in the earlier analysis, the column parameters were matched to the particular class of compounds being analyzed.

TABLE 5. COMPOSITION OF STANDARD MIXTURE* USED IN ORGANICS ANALYSIS

Compound	Concentration (µg/ml)
benzaldehyde	104.2
benzonitrile	101.0
o-toluenitrile	98.1
4-cyanopyridine	96.7
nitrobenzene	120.4
3-cyanopyridine	97.0
benzylcyanide	101.6
phenol	103.5
eicosane	99.0
1,4-dicyanobenzene	263.7
1,2-dicyanobenzene	96.7
tetracosane	12.4
benzamide	128.6
pyrene	127.1
dodecane (internal standard)	74.9

*In methylene chloride (CH_2Cl_2) solution.

In a typical analysis, the magnet of the mass spectrometer was set to scan repetitively over a pre-set mass range. Data were acquired on a disk by the data system and stored on magnetic tape for subsequent examination. The raw GC/MS data was then routinely processed through a data-enhancement algorithm. Program "Clean-up"* automatically extracted mass spectra free of background and of contributions of unresolved (overlapping) GC peaks by the application of tabular peak-modeling technique to mass chromatograms in the data file (Rindfleisch deconvolution). The resolved spectra were then identified by means of a library-matching search algorithm. Compounds which did not yield acceptable identifications in this way were sought manually by comparison of their spectra with published compendia of mass spectral data.

---

*Developed at Stanford University Medical School and modified at IITRI.

5. RESULTS OF ANALYSIS

5.1 ELEMENTAL ANALYSIS OF FELT WEDGE MATERIAL

Samples of phosphorus-free felt wedges were sent to Phoenix Laboratories, Chicago, Illinois for elemental analysis. The results are summarized in Table 6.

5.2 TRACE METAL ANALYSIS OF PURE PHOSPHORUS

A sample of army-supplied phosphorus was sent to T.E.I. Analytical Laboratories, Park Ridge, Illinois for trace metal analysis. The results of the analysis are listed in Table 7.

5.3 RESULTS OF PRELIMINARY ANALYSIS

Smoldering Felt Smoke

The felt smoke was analyzed by capillary gas chromatography but no effort was made to identify the species present. The chromatographic trace of the felt smoke bore no resemblance to the trace obtained from the munition smoke. It is believed that the felt smoke did not represent the composition of the organic species in the munition and further analysis was not pursued. A representative chromatogram of the felt smoke is shown in Figure 5.

Thin Layer Chromatography Analysis of Munition Smoke

TLC analysis demonstrated that the acid composition of the munition smoke consisted of a set of polyphosphoric acids through at least polymer number eight. Phosphinic acid, phosphorous acid and metaphosphoric acids were never positively detected even though the TLC system was capable of separating and detecting them. A representation of a developed TLC plate is shown in Figure 6.

Analysis of Phosphorus in Smoke Produced in Small Reactor

Twenty-eight experiments were performed in which the unburned phosphorus content of the munition smoke was determined. Various experimental conditions

TABLE 6. ELEMENTAL ANALYSIS OF FELT WEDGE MATERIAL

	% (weight)
Carbon	48.32
Hydrogen	7.58
Sulfur	2.75
Nitrogen	14.09
Ash	0.78
Phosphorus	<0.01
Total Halogens (as chlorine)	0.26
Oxygen (by difference)	26.22

TABLE 7. TRACE METAL ANALYSIS OF PHOSPHORUS

Aluminum	20.00 ppm	Iron	94.00
Arsenic	84.00	Lead	1.28
Barium	0.45	Magnesium	3.60
Boron	715.00	Manganese	0.58
Cadmium	0.88	Molybdenum	0.09
Calcium	18.30	Nickel	0.96
Chromium	0.49	Silicon	377.00
Cobalt	0.57	Sodium	9.50
Copper	1.22	Vanadium	4.20
		Zinc	0.88

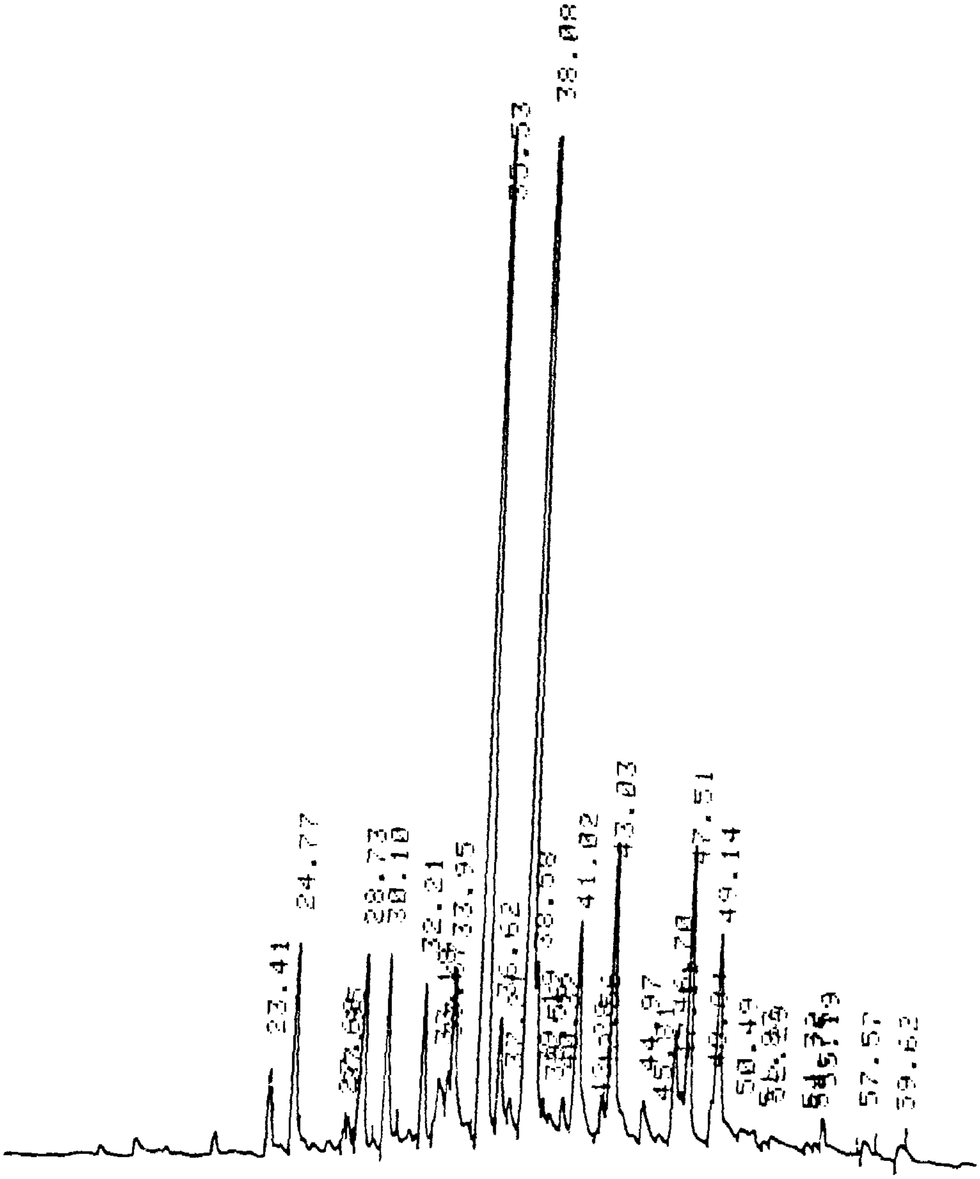

Figure 5. Gas chromatographic trace of organics collected from smoldering felt smoke.

S0: conc. NH_3 soln / methanol / isobutanol / water (9:50:10:31)

S2: isopropanol / water / 20% trichloroacetic acid soln / conc. NH_3 soln. (70:10:20:0.3)

Visualizing solution: ammonium molybdate reagent + U.V. light

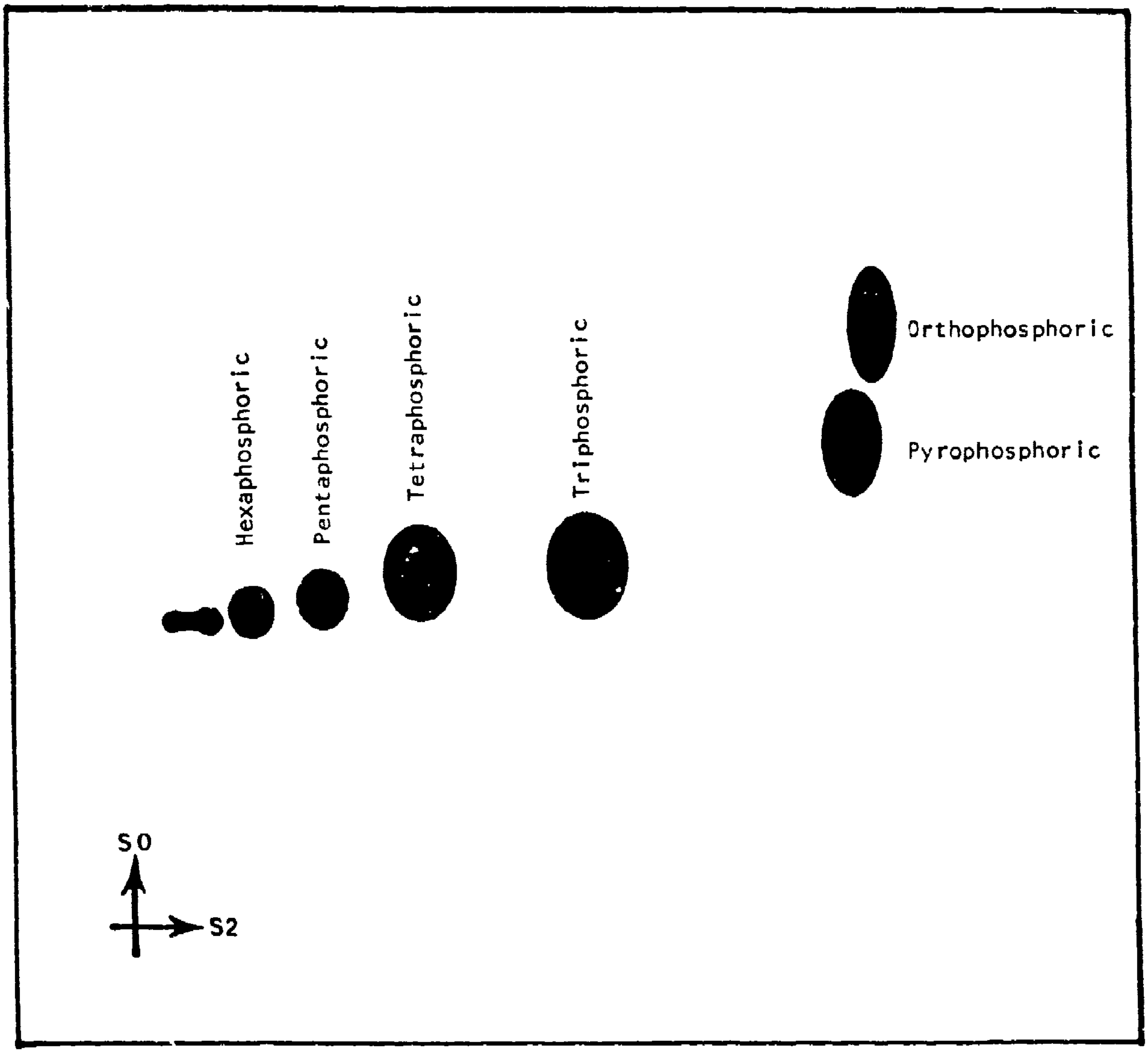

Figure 6. TLC (cellulose) of acids collected from burning phosphorus munition in air, 50% relative humidity.

were utilized but no positive relationship between conditions and results was ever realized. In fact, the results varied over a very large range perhaps due to the variations in the compositions of the pieces of munition burned. It appeared visually that some pieces contained more phosphorus than others. A summary of experimental conditions and results appears in Table 8.

It should be noted that the time period between smoke generation and trapping in o-xylene is on the order of a few seconds. The effects of smoke aging on the smoke's phosphorus content are unknown.

5.4 RESULTS OF ANALYSIS USING SMOKE GENERATED FROM LARGE REACTOR

Introduction

A total of 18 experiments was run using the large reactor under a variety of conditions. The experimental conditions and experiment numbers are compiled in Table 9.

TABLE 9. EXPERIMENT NUMBERS AND EXPERIMENTAL CONDITIONS USING LARGE REACTOR SYSTEM

	Air Flow Rate		
Humidity	2 Liters-min^{-1}	4 Liters-min^{-1}	8 Liters-min^{-1}
33.3%	*	29, 30, 42N	34
50.0%	35, 36	25, 26, 27, 31, 37N, 38T, 39B, 40B,	32
66.7%	*	28, 41N	

* Signifies conditions outside the capabilities of the system.

N Signifies experiments in which 5 ppm (v) NH_3 was added to the air flow.

B Signifies blank experiments in which no munition was burned but sample collection and analysis were performed.

T Signifies an experiment in which hydrolysis of the polyphosphoric acids collected was monitored for several days.

TABLE 8. SUMMARY OF ANALYSIS OF UNBURNED PHOSPHORUS IN MUNITION SMOKE

Expt. No.	Humidity (%)	Air Flow Rate (ml-min^{-1})	Wt. Phosphorus Detected/ Wt. Munition Burned	Means
7	50.0	400	2.66×10^{-3}	
8	50.0	400	8.70×10^{-4}	
9	50.0	400	$<4.8 \times 10^{-7}$	
10	50.0	400	5.02×10^{-3}	2.14×10^{-3}
11	50.0	800	8.69×10^{-3}	
12	50.0	800	1.23×10^{-5}	
13	50.0	800	$<5.5 \times 10^{-7}$	
14	50.0	800	2.27×10^{-5}	2.18×10^{-3}
15	62.5	800	2.13×10^{-3}	
16	62.5	800	4.66×10^{-3}	
17	62.5	800	3.06×10^{-2}	
18	62.5	800	1.45×10^{-2}	1.30×12^{-2}
19	37.5	800	3.65×10^{-4}	
20	37.5	800	6.27×10^{-5}	
21	37.5	800	9.50×10^{-6}	
22	37.5	800	2.44×10^{-4}	2.24×10^{-2}
23	37.5	400	1.93×10^{-2}	
24	37.5	400	1.39×10^{-5}	
25	37.5	400	5.45×10^{-3}	
26	37.5	400	6.26×10^{-3}	7.76×10^{-3}
27	62.5	400	1.58×10^{-3}	
28	62.5	400	1.78×10^{-2}	
29	62.5	400	3.81×10^{-3}	
30	62.5	400	2.90×10^{-3}	6.52×10^{-3}
31*	50.0	800	5.47×10^{-4}	
32*	50.0	800	5.92×10^{-6}	
33*	50.0	800	2.31×10^{-5}	
34*	50.0	800	4.93×10^{-2}	1.25×10^{-2}
Median			2.39×10^{-3}	
Minimum			$<4.8 \times 10^{-7}$	
Maximum			4.93×10^{-2}	

*5 ppm (v) NH_3 was added to the air flow in these experiments.

Polyphosphoric Acid Results

Using the anion exchange HPLC system described previously it was possible to separate and quantitate the polyphosphoric acids present in the smoke as orthophosphoric acid. Quantitation and presentation of the results required several assumptions. The CFA 200 Autoanalyzer* system used to quantitate the acids operated colorimetrically by producing and measuring a colored derivative of orthophosphoric acid. In order to measure the levels of the larger acids it was necessary to hydrolize those acids to orthophosphoric acid. The instrument manual indicated that the hydrolysis was 90% effective. However, experiments with sodium pyrophosphate using the complete HPLC/CFA-200 system showed that the system was only 80% effective. Attempts to improve this value by introducing nitric acid into the system failed as the nitric acid destroyed the colored derivative necessary for detection. It was not possible to measure the degree of hydrolysis of the larger acids due to the difficulty in obtaining these compounds in a pure form. Therefore, in calculating results it was assumed that all the polyphosphoric acids were only 80% hydrolyzed in the analyzer and corrections were made to obtain the final results.

Total weight of munition burned could be determined in two ways. The most straightforward method was simply to weigh the munition before and after the experiment. However, the ash remaining was coated with oxidized material which affected the results and cast doubt upon the measurement. As an alternative, the total amount of phosphorus collected (which should equal the total burned) could be calculated by measuring the orthophosphoric acid content of a sample in which the acids were completely hydrolyzed by using concentrated nitric acid and heating. If it is assumed that an average piece of munition contains 80% phosphorus by weight (an average number obtained by comparing the weight of felt with the weight of munition) a value for the weight of munition burned could be calculated. In practice, the values obtained by both methods were usually close, however, the values obtained from the second method were used in calculating final results. Somewhat surprisingly, only about 40% of the phosphorus burned in any given experiment, the rest remaining trapped within the residue material.

---

*Manufactured by Technicon, Inc.

The distribution of the polyphosphoric acids in the smoke is presented in Figure 7 in terms of weight of acid produced divided by weight of munition burned. There was a fairly large spread in the data, so the data have been presented as maximum, median, and minimum experimental values. Detailed results of all experiments are summarized in Table 10. No obvious relationship was identified between the experimental conditions and the final results.

Figure 8 represents a slightly different view of the acid distribution. Here the acids are presented in terms of the phosphorus distribution in the smoke. It is immediately obvious that 38% of the total phosphorus was present in acids larger than octaphosphoric. Our system was not capable of the analysis of these large acids and the percentage was arrived at by calculating the difference between the total phosphorus collected and the phosphorus present in the analyzed acids.

To help confirm the existence of the larger acids and to gain some insight into the stability of the acids against hydrolysis, an aqueous solution of the smoke produced from Expt. 38 was analyzed periodically over a period of eight days. The results are summarized in Table 11 and are plotted in Figure 9. As expected, the larger acids reached their maximum value early as hydrolysis produced successively smaller acids. The curve behaviors and continuing increase in total measurable acids provides good evidence for the initial existence of the larger acids. Also, the relative short term stability of the acid mixture creates confidence that the initial acid analysis of each experiment is an unaltered reflection of the material collected. It should be noted, however, that the effects of cryogenic collection on the composition of the smoke material is unknown.

Results of Gas and Organic Analysis

A typical chromatogram of an organic analysis is shown in Figure 10 and is keyed in Table 12.

The measured values for all organics and gases analyzed are summarized in detail in Table 10 and are presented graphically in Figure 11. As with the polyphosphoric acids, no positive correlation could be established between

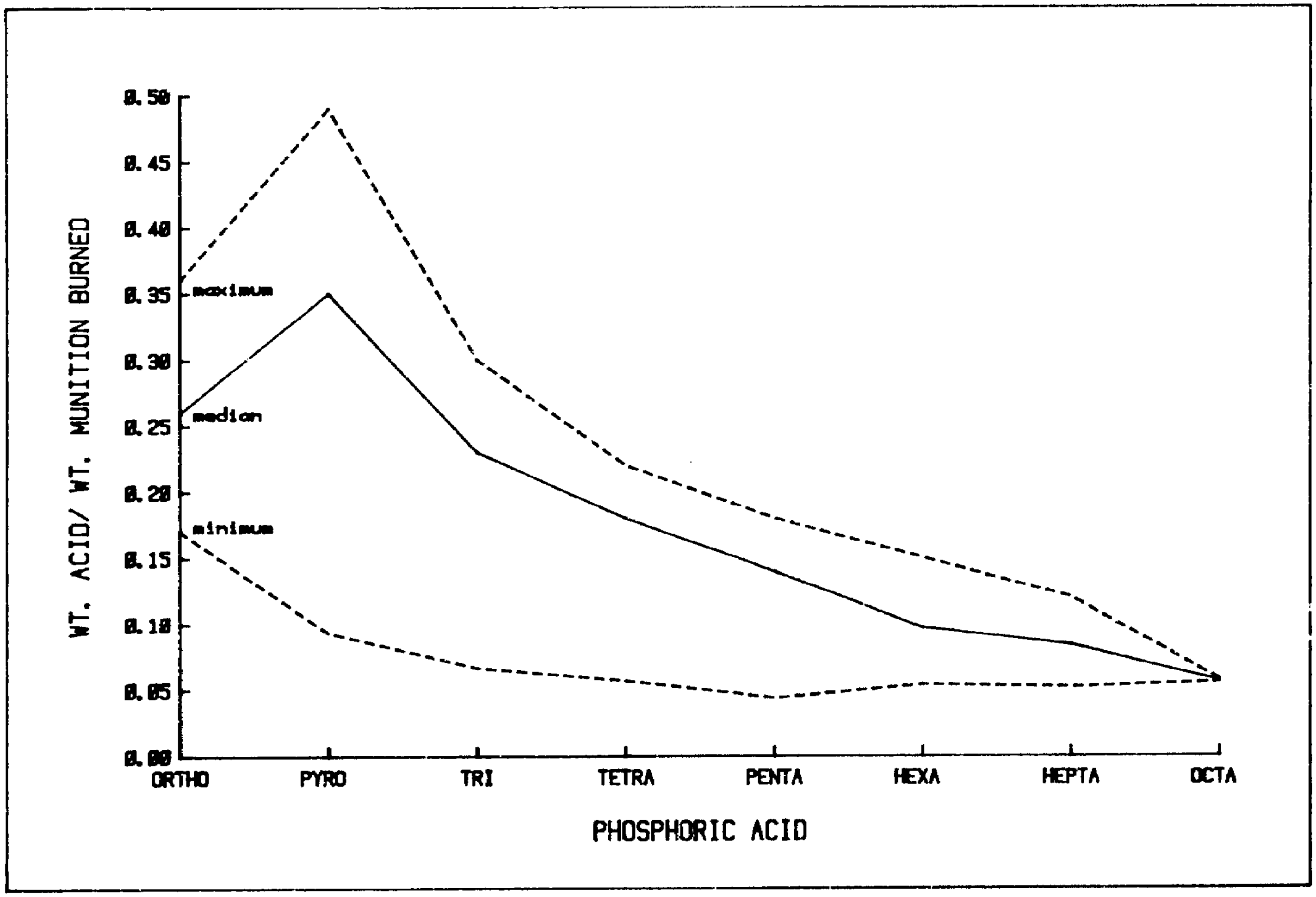

Figure 7. Distribution of resolvable polyphosphoric acids in smoke.

TABLE 10. SUMMARY OF ANALYTICAL RESU

Air Flow Rate →		2 Liters-Min⁻¹		4 Liters-Min.⁻¹						
Humidity →		50.0%		33.3%			50.0%			
Compound	M.W.	35	36	29	30	42N	25	26	27	
orthophosphoric acid	98.00	3.1 E-1	2.3 E-1	2.6 E-1	3.0 E-1	-	2.0 E-1	2.7 E-1	1.7 E-1	3.5
pyrophosphoric acid	177.98	4.4 E-1	3.2 E-1	-	3.9 E-1	-	9.3 E-2	4.5 E-1	2.0 E-1	4.4
tripolyphosphoric acid	257.95	2.8 E-1	2.1 E-1	2.8 E-1	2.6 E-1	2.2 E-1	6.7 E-2	2.4 E-1	1.4 E-1	2.8
tetrapolyphosphoric acid	337.93	2.2 E-1	1.0 E-1	1.8 E-1	2.0 E-1	1.9 E-1	5.7 E-2	1.9 E-1	1.4 E-1	1.8
pentapolyphosphoric acid	417.91	1.7 E-1	7.5 E-2	1.4 E-1	1.3 E-1	1.7 E-1	4.4 E-2	1.5 E-1	1.4 E-1	1.2
hexapolyphosphoric acid	497.89	1.3 E-1	6.2 E-2	9.4 E-2	7.5 E-2	1.5 E-1	5.4 E-2	1.2 E-1	1.2 E-1	8.6
heptapolyphosphoric acid	577.87	7.5 E-2	5.8 E-2	6.9 E-2	7.0 E-2	1.2 E-1	5.2 E-2	9.5 E-2	7.7 E-2	7.3
octapolyphosphoric acid	657.85	5.6 E-2	-	5.8 E-2	-	-	-	-	-	-
hydrogen	2.02	5.6 E-4	2.0 E-4	2.3 E-4	5.0 E-4	3.2 E-4	8.5 E-5	-	2.5 E-4	1.2
carbon monoxide	28.01	1.6 E-2	1.0 E-3	1.3 E-2	2.3 E-2	1.8 E-2	7.8 E-3	-	3.8 E-3	8.6
carbonyl sulfide	76.14	2.3 E-4	2.5 E-5	7.6 E-5	2.6 E-4	1.3 E-4	<2 E [illegible]	-	1.0 E-4	1.0
phosphine	34.00	3 E-7	-	<2 E-7	<2 E-7	<2 E-7	<1 E-7	-	-	<2
hydrogen cyanide	27.03	4.9 E-5	-	2.2 E-4	2.8 E-4	2.8 E-6	5.8 E-5	-	-	2.1
methane	16.04	-	-	1.7 E-4	3.8 E-4	-	-	-	-	2.4
acetylene	26.04	-	-	8.8 E-5	1.6 E-4	-	-	-	-	9.5
ethylene	28.05	-	-	5.0 E-5	2.5 E-4	-	-	-	-	1.7
propylene	42.08	1.3 E-5	2 E-6	<2 E-6	2.6 E-5	<6 E-7	<1 E-6	-	5.8 E-6	2.4
acetonitrile	41.05	7 E-7	-	-	1.7 E-5	<5 E-7	3.3 E-6	-	-	<4
acrylonitrile	53.06	9 E-7	-	-	2.1 E-5	<6 E-7	2.5 E-6	-	-	<5
propionitrile	55.08	9 E-7	-	<4 E-7	<7 E-7	<6 E-7	<2 E-7	-	-	<5
benzamide	121.14	4 E-7	3 E-7	<4 E-7	<4 E-7	<4 E-7	5.8 E-7	<3 E-7	1.6 E-6	1.3
nitrobenzene	123.11	4 E-7	3 E-7	<4 E-7	<4 E-7	<4 E-7	3.5 E-7	6.9 E-7	4.7 E-7	3.5
benzomitrile	103.13	9.3 E-7	3 E-7	<4 E-7	<4 E-7	<4 E-7	<4 E-7	<3 E-7	4.6 E-7	4.8
benzylcyanide	117.15	4 E-7	3 E-7	<4 E-7	<4 E-7	<4 E-7	6.9 E-7	7.0 E-7	3.9 E-7	4.9
1,2-dicyanobenzene	128.14	1.5 E-5	5.0 E-6	2.2 E-6	3.9 E-6	2.8 E-6	2.4 E-6	1.2 E-6	4.0 E-6	1.6
1,3-dicyanobenzene	128.14	3.6 E-5	2.6 E-6	1.6 E-6	6.9 E-6	7.7 E-6	5.7 E-6	2.6 E-6	5.4 E-6	3.2
1,4-dicyanobenzene	128.14	8.6 E-5	3.4 E-5	3.0 E-5	1.1 E-4	5.6 E-5	5.2 E-5	3.2 E-5	1.0 E-4	6.6

SUMMARY OF ANALYTICAL RESULTS, UNITS IN WT. COMPOUND/WT. MUNITION BURNED

	4 Liters-Min.$^{-1}$							8 Liters-Min.$^{-1}$					
	50.0%					66.7%		33.3%	50.0%	66.7%			
	26	27	31	38T	37N	28	41N	34	32	33	Median	Minimum	Maximum
-1	2.7 E-1	1.7 E-1	3.5 E-1	2.2 E-1	3.4 E-1	2.6 E-1	3.2 E-1	2.1 E-1	3.6 E-1	2.3 E-1	2.60 E-1	1.7 E-1	3.6 E-1
-2	4.5 E-1	2.0 E-1	4.4 E-1	3.1 E-1	4.9 E-1	3.4 E-1	3.5 E-1	3.6 E-1	2.9 E-1	3.0 E-1	3.50 E-1	9.3 E-2	4.9 E-1
-2	2.4 E-1	1.4 E-1	2.8 E-1	1.9 E-1	3.0 E-1	2.4 E-1	1.8 E-1	2.2 E-1	2.1 E-1	2.3 E-1	2.30 E-1	6.7 E-2	3.0 E-1
-2	1.9 E-1	1.4 E-1	1.8 E-1	1.4 E-1	2.1 E-1	1.9 E-1	1.5 E-1	1.8 E-1	1.6 E-1	1.7 E-1	1.80 E-1	5.7 E-2	2.2 E-1
-2	1.5 E-1	1.4 E-1	1.2 E-1	1.3 E-1	1.6 E-1	1.8 E-1	1.5 E-1	1.3 E-1	1.2 E-1	1.2 E-1	1.40 E-1	4.4 E-2	1.8 E-1
-2	1.2 E-1	1.2 E-1	8.6 E-2	8.1 E-2	1.2 E-1	1.3 E-1	7.9 E-2	9.3 E-2	1.1 E-1	1.0 E-1	9.70 E-2	5.4 E-2	1.5 E-1
-2	9.5 E-2	7.7 E-2	7.3 E-2	8.0 E-2	9.9 E-2	1.1 E-1	8.8 E-1	9.2 E-1	9.2 E-1	8.9 E-1	8.40 E-2	5.2 E-2	1.2 E-1
	-	-	-	-	-	-	-	-	-	-	5.70 E-2	5.6 E-2	5.8 E-2
-5	-	2.5 E-4	1.2 E-4	-	3.5 E-4	5.2 E-4	4.2 E-4	2.1 E-4	4.3 E-4	-	3.20 E-4	8.5 E-5	5.6 E-4
-3	-	3.8 E-3	8.6 E-4	-	9.5 E-3	1.4 E-2	1.7 E-2	1.0 E-2	2.9 E-2	-	1.30 E-2	8.6 E-4	2.9 E-2
-6	-	1.0 E-4	1.0 E-4	-	-	4.4 E-4	2.1 E-4	<4 E-6	2.4 E-4	-	1.15 E-4	<2 E-6	4.4 E-4
-7	-	-	<2 E-7	-	<2 E-7	<2 E-7	<3 E-7	<3 E-7	<2 E-7	-	<2 E-7	<3 E-7	<1 E-7
-5	-	-	2.1 E-4	-	5.4 E-5	7.1 E-5	4.6 E-5	3.9 E-5	2.9 E-4	-	5.80 E-5	2.8 E-6	2.9 E-4
	-	-	2.4 E-4	-	-	2.3 E-4	-	8.0 E-5	2.8 E-4	-	2.35 E-4	8.0 E-5	3.8 E-4
	-	-	9.5 E-5	-	-	<6 E-5	-	<9 E-5	1.6 E-4	-	9.15 E-5	<6 E-5	1.6 E-4
	-	-	1.7 E-4	-	-	2.3 E-4	-	<9 E-5	1.5 E-4	-	1.60 E-4	5.0 E-5	2.5 E-4
-6	-	5.8 E-6	2.4 E-5	-	-	2.7 E-5	1.7 E-5	<3 E-6	9.5 E-6	-	7.65 E-6	<6 E-7	2.7 E-5
-6	-	-	<4 E-7	-	-	<2 E-7	<2 E-7	<6 E-7	2.9 E-5	-	<6 E-7	<2 E-7	2.9 E-5
-6	-	-	<5 E-7	-	<5 E-7	<3 E-7	<7 E-7	<7 E-7	6.0 E-6	-	<7 E-7	<3 E-7	2.1 E-5
-7	-	-	<5 E-7	-	<6 E-7	<3 E-7	<7 E-7	<7 E-7	<7 E-7	-	<6 E-7	<2 E-7	<9 E-7
-7	<3 E-7	1.6 E-6	1.3 E-6	-	3.7 E-6	1.8 E-6	<3 E-7	<3 E-7	<3 E-7	<3 E-7	<4 E-7	<3 E-7	3.7 E-6
-7	6.9 E-7	4.7 E-7	3.5 E-7	-	1.9 E-6	2.8 E-7	<3 E-7	5.7 E-7	<3 E-7	<3 E-7	<4 E-7	<3 E-7	1.9 E-6
-7	<3 E-7	4.6 E-7	4.8 E-7	-	6.1 E-7	2.3 E-7	<3 E-7	<3 E-7	<3 E-7	<3 E-7	<4 E-7	<3 E-7	9.3 E-7
-7	7.0 E-7	3.9 E-7	4.9 E-7	-	2.5 E-6	3.3 E-7	<3 E-7	4.0 E-7	<3 E-7	<3 E-7	<4 E-7	<3 E-7	2.5 E-6
6	1.2 E-6	4.0 E-6	1.6 E-6	-	6.2 E-6	2.6 E-6	1.4 E-5	2.8 E-6	1.7 E-6	8.9 E-7	2.8 E-6	8.9 E-7	1.5 E-5
6	2.6 E-6	5.4 E-6	3.2 E-6	-	1.2 E-5	3.8 E-6	3.3 E-5	6.4 E-6	1.9 E-6	2.9 E-6	5.4 E-6	1.6 E-6	3.6 E-5
6	3.2 E-5	1.0 E-4	6.6 E-5	-	2.4 E-4	1.0 E-4	1.8 E-4	2.7 E-5	2.9 E-5	3.4 E-5	5.6 E-5	2.7 E-5	2.4 E-4

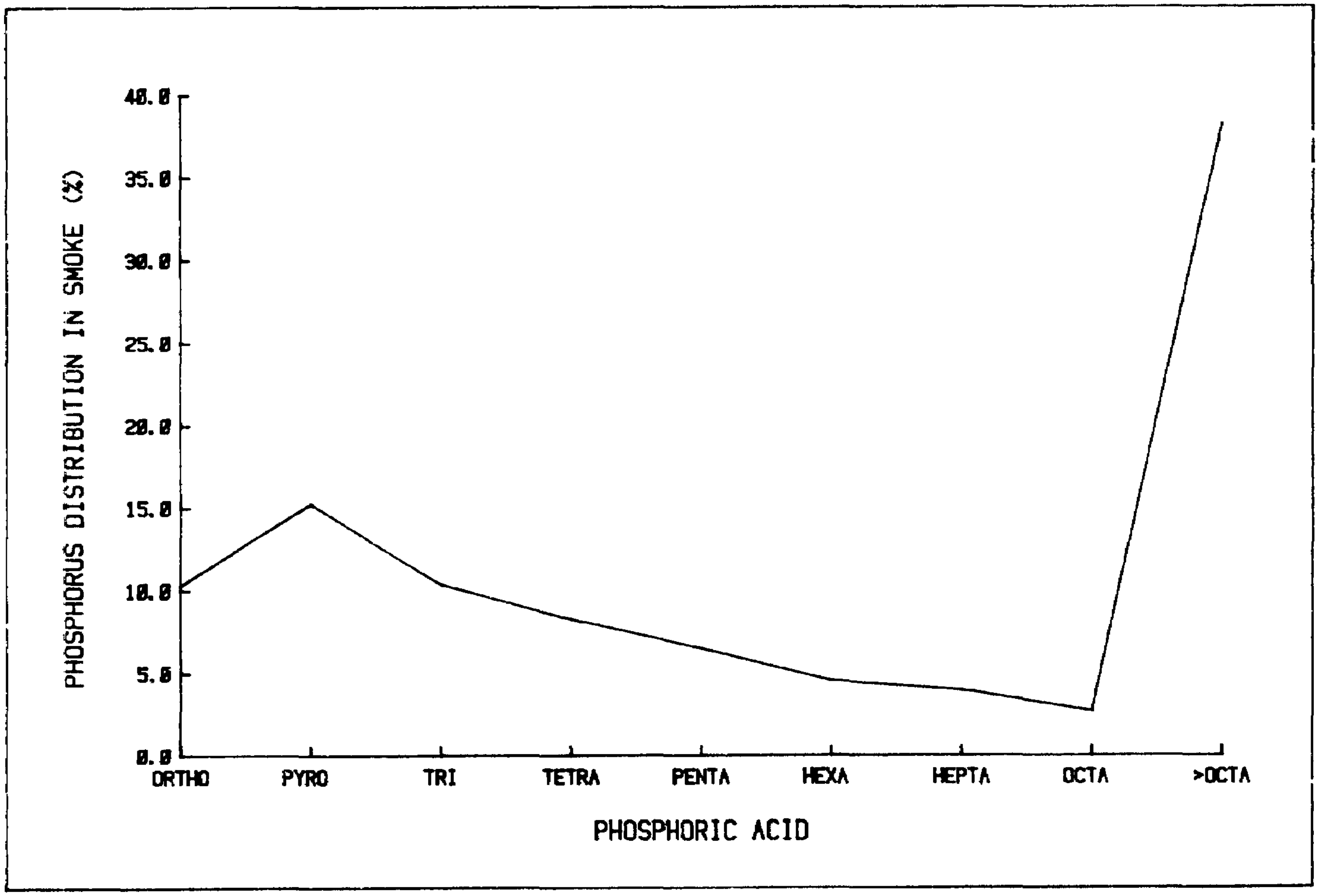

Figure 8. Median values of phosphorus distribution in smoke.

TABLE 11. HYDROLYSIS OF POLYPHOSPHORIC ACIDS FROM SMOKE

(Units in wt. Acid Produced/wt. Munition Burned)

	Day 0	Day 1	Day 2	Day 3	Day 8
Orthophosphoric Acid	0.224	0.581		0.793	
Pyrophosphoric Acid	0.307	0.626		0.713	
Tripolyphosphoric Acid	0.187	0.360	0.497	0.446	0.252
Tetrapolyphosphoric Acid	0.140	0.298	0.315	0.231	0.079
Pentapolyphosphoric Acid	0.129	0.200	0.192	0.101	0
Hexapolyphosphoric Acid	0.081	0.207	0.107	0.055	0
Heptapolyphosphoric Acid	0.080	0.139	0.074	0.032	0

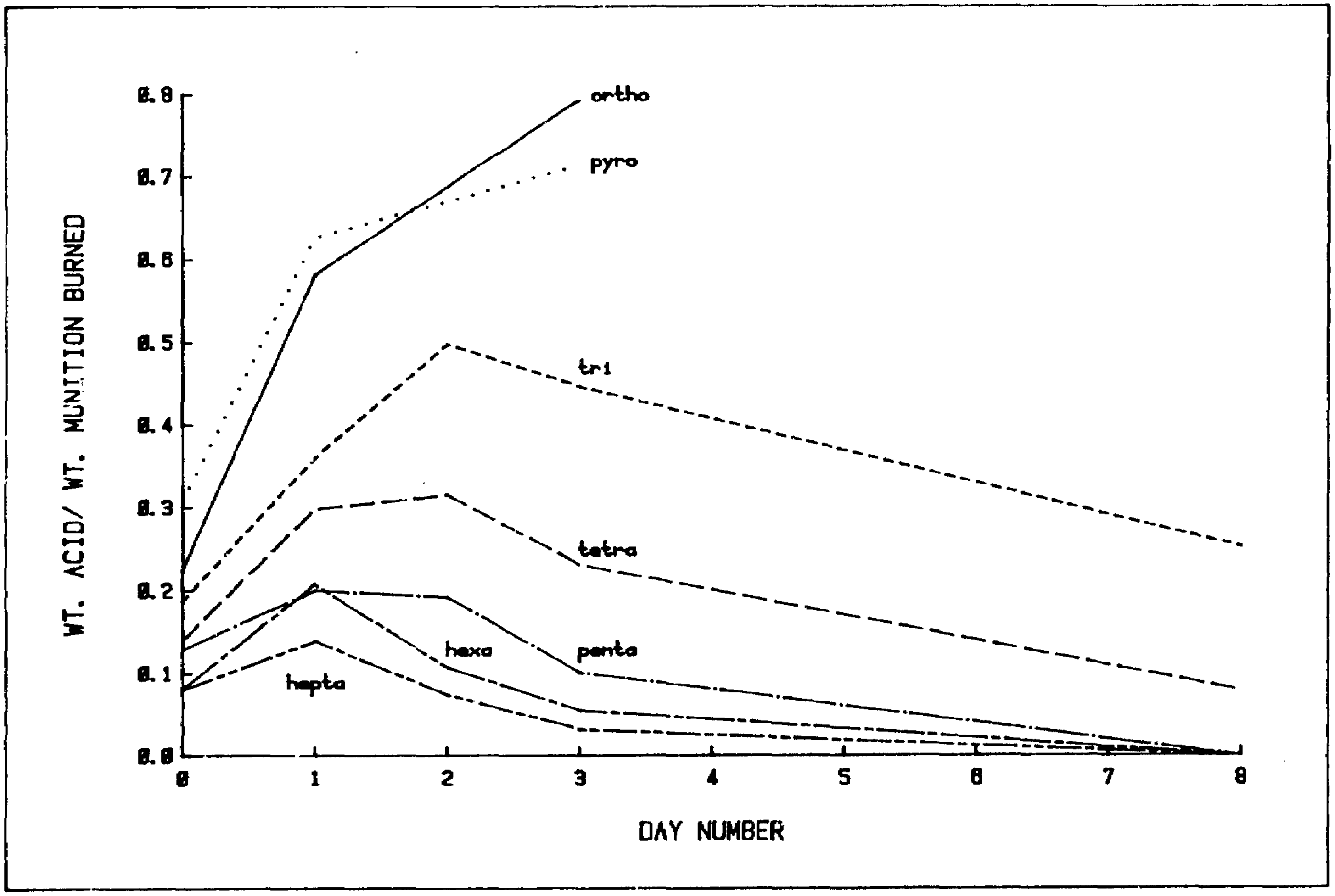

Figure 9. Hydrolysis of acid mixture from experiment 38.

TABLE 12. KEY TO CHROMATOGRAM IN FIGURE 10

A.	dodecane (internal standard)
B.	benzonitrile
C.	nitrobenzene
D.	benzylcyanide
E.	1,4-dicyanobenzene
F.	1,3-dicyanobenzene
G.	1,2-dicyanobenzene
H.	benzamide
I.	pyrene (reference standard)

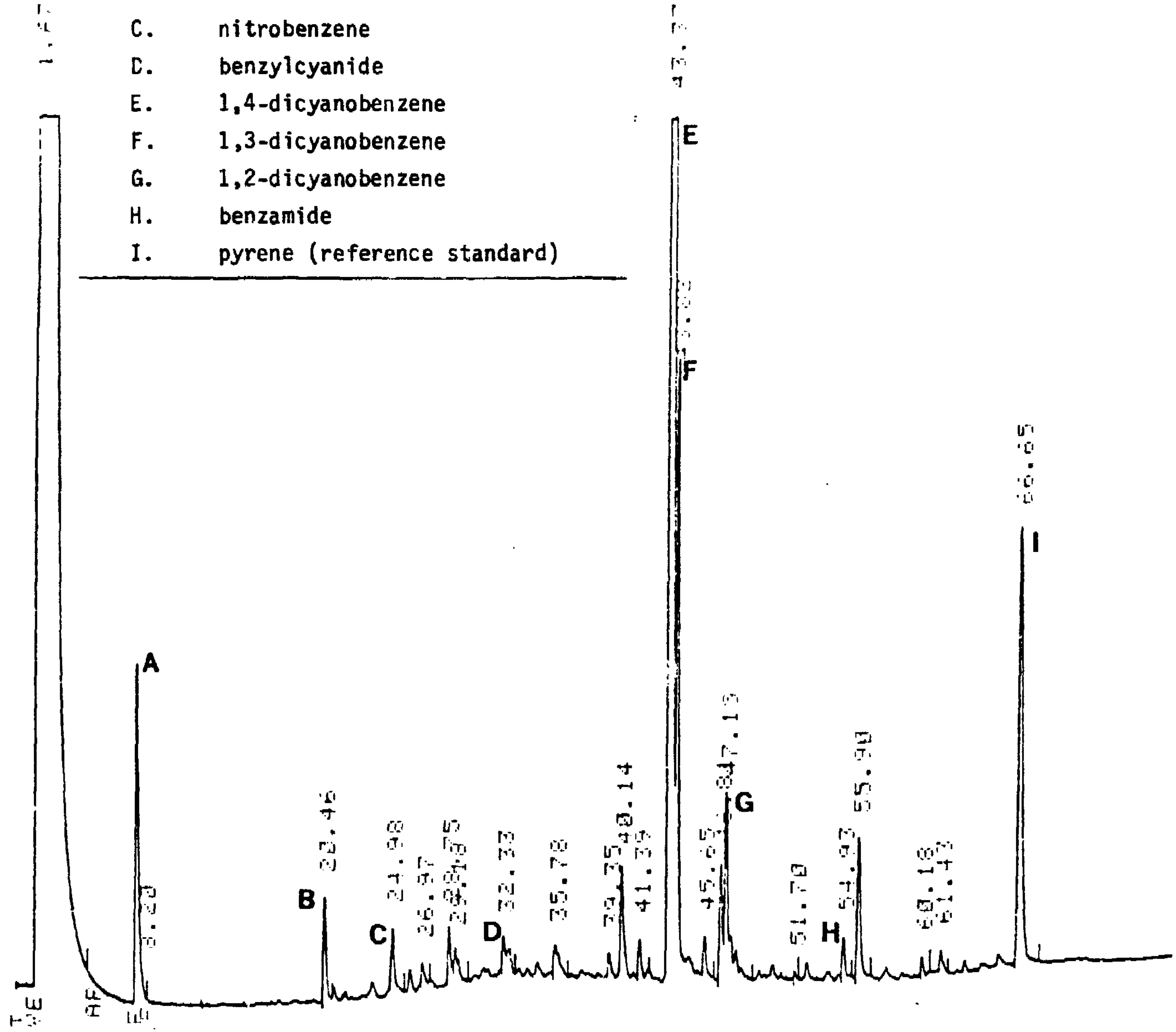

Figure 10. Typical gas chromatographic trace of organics collected from munition smoke.

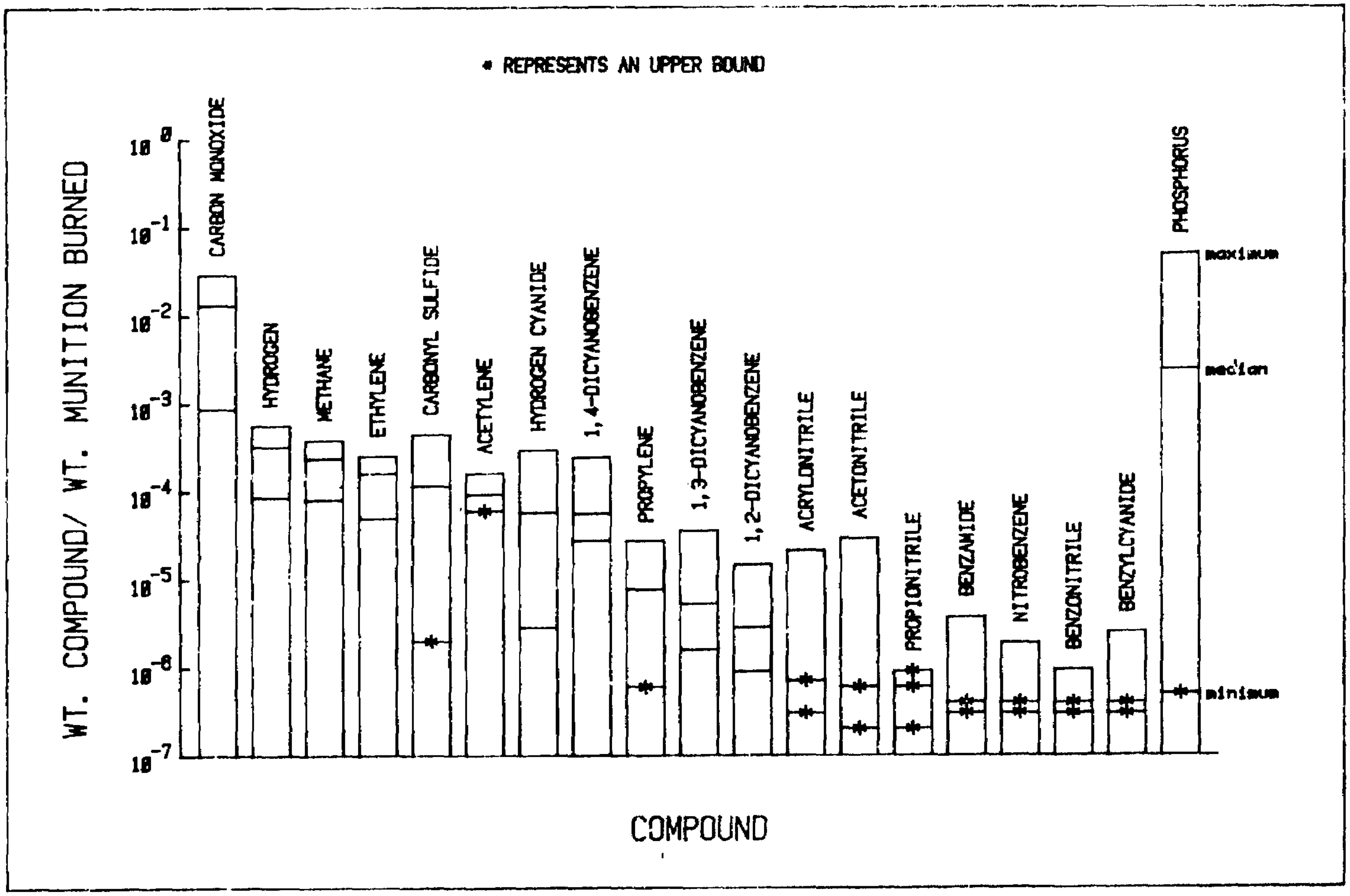

Figure 11. Bar graph of analytical results for organics and light compounds.

experimental condition and analytical result. In some cases it was possible only to obtain an upper limit and those values are noted as such. All results displayed in Figure 11 were obtained from experiments carried out in the large reactor with the exception of phosphorus. Uncertainties in the phosphorus analysis have been described previously. A few compounds were detected by GC/MS but analytical problems prevented them from being quantitated. Those compounds are listed in Table 13.

Using median and maximum measured values, the vapor phase concentration of compounds found in the smoke have been calculated at three smoke densities and are summarized in Table 14.

TABLE 13. COMPOUNDS DETECTED AND IDENTIFIED BY GC/MS BUT NOT QUANTIFIED

sulfur dioxide
cyanopyridine isomers
cyanotoluene isomers
nitrotoluene isomers
vinylidene cyanide
napthonitrile isomers
quinoline
propyne
allene
carbon disulfide

TABLE 14. CALCULATED CONCENTRATIONS OF VARIOUS COMPOUNDS AT THREE DIFFERENT SMOKE DENSITIES (UNITS IN ppb (v) UNLESS OTHERWISE STATED)

Smoke Density →	0.1 g/m^3		0.5 g/m^3		1.0 g/m^3	
	Median	Maximum	Median	Maximum	Median	Maximum
carbon monoxide	520	1.2 ppm	2.6 ppm	5.8 ppm	5.2 ppm	12 ppm
phosphorus	21	440	110	2.2 ppm	220	4.4 ppm
hydrogen	180	310	880	1.5 ppm	1.8 ppm	3.1 ppm
methane	16	26	81	130	160	260
ethylene	6	10	32	50	63	99
carbonyl sulfide	2	6	8	32	17	64
acetylene	4	7	20	34	39	68
hydrogen cyanide	2	12	12	60	24	120
1,4-dicyanobenzene	<1	2	2	10	5	21
propylene	<1	1	1	4	2	7
1,3-dicyanobenzene	<1	<1	<1	2	<1	3
1,2-dicyanobenzene	<1	<1	<1	1	<1	1
acrylonitrile	<1	<1	<1	2	<1	4
acetonitrile	<1	<1	<1	4	<1	8
propionitrile	<1	<1	<1	<1	<1	<1
benzamide	<1	<1	<1	<1	<1	<1
nitrobenzene	<1	<1	<1	<1	<1	<1
benzonitrile	<1	<1	<1	<1	<1	<1
benzylcyanide	<1	<1	<1	<1	<1	<1
phosphine	<1	<1	<1	<1	<1	<1

6. WHITE PHOSPHORUS-FELT MUNITION AEROSOL CHARACTERIZATION

6.1 PROCEDURE AND INSTRUMENTATION

The phosphorus smoke aerosols were generated by allowing a known weight of phosphorus-felt munition to react in a 2 m^3 rectilinear chamber 1 m x 1 m x 2 m high. The humidity in the chamber was controlled externally. Humidities higher than the ambient were achieved by mixing dry and saturated air in the chamber. Lower humidities were achieved by spreading silica gel crystals at the bottom of the chamber and leaving them overnight. The felt munition usually ignited spontaneously as soon as it was released in the chamber. Manipulating the munition with a metal rod to expose fresh surfaces helped ignition. A fan at the bottom of the chamber distributed the aerosol through the chamber. The experimental arrangement is shown in Figure 12.

The aerosol was drawn from the holding chamber with dilution at successive intervals to observe particle size and concentration and the effects of aging on the aerosols. The aerosol dilution system is shown in Figure 13. An important function of this system was the reduction of the chamber aerosol concentration to a level suitable for measurement by the two aerosol monitors. A dilution of 1000 (±10):1 was used with a total transit time from chamber to detector of somewhat less than 1 min. A feature of the system is the use of recirculated air for dilution to preserve the physical characteristics of the sample. The aerosol particles were analyzed using the two instruments described below.

A California Measurements, Inc. Piezo-Electric (P/Z) Particle Cascade Impactor Model PC-Z was used for the direct measurement of the mass concentration of air-suspended particles between 0.05 and 25μm. The aerosol-laden air stream, sampled at 240 ml/min, is impacted sequentially on 10 quartz crystal impactor stages. The mass accumulated by each stage causes a proportional frequency shift on each impactor crystal, which is electronically compared to a matching clean reference crystal. Table 15 lists the 50% cutoff sizes (D_p50) for the ten stages for a particle density of 2 g cm^{-3}. The values of M_i are the between-stage midpoint diameters used to compute the aerodynamic equivalent mass median diameters for each distribution.

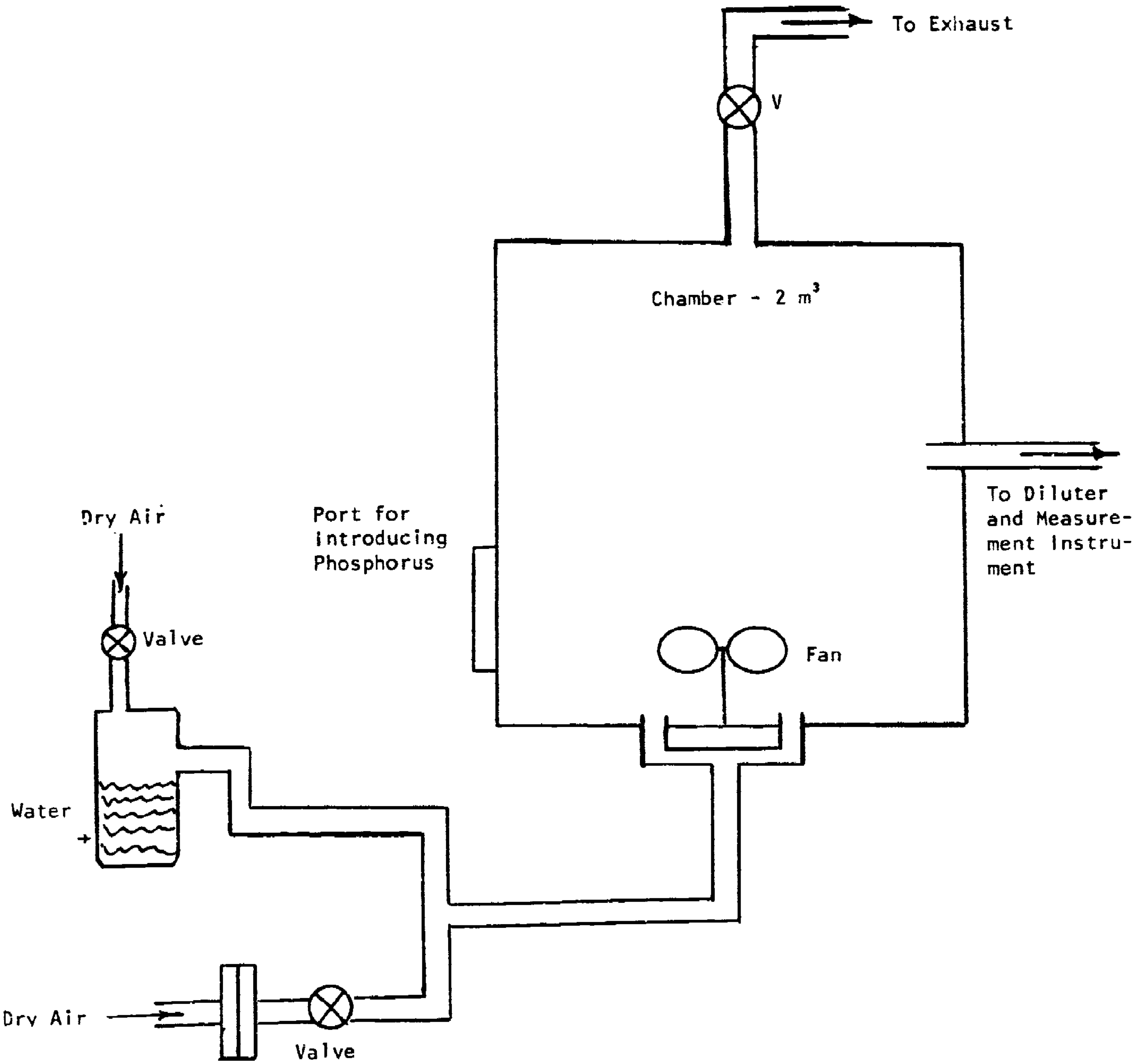

Figure 12. Aerosol chamber.

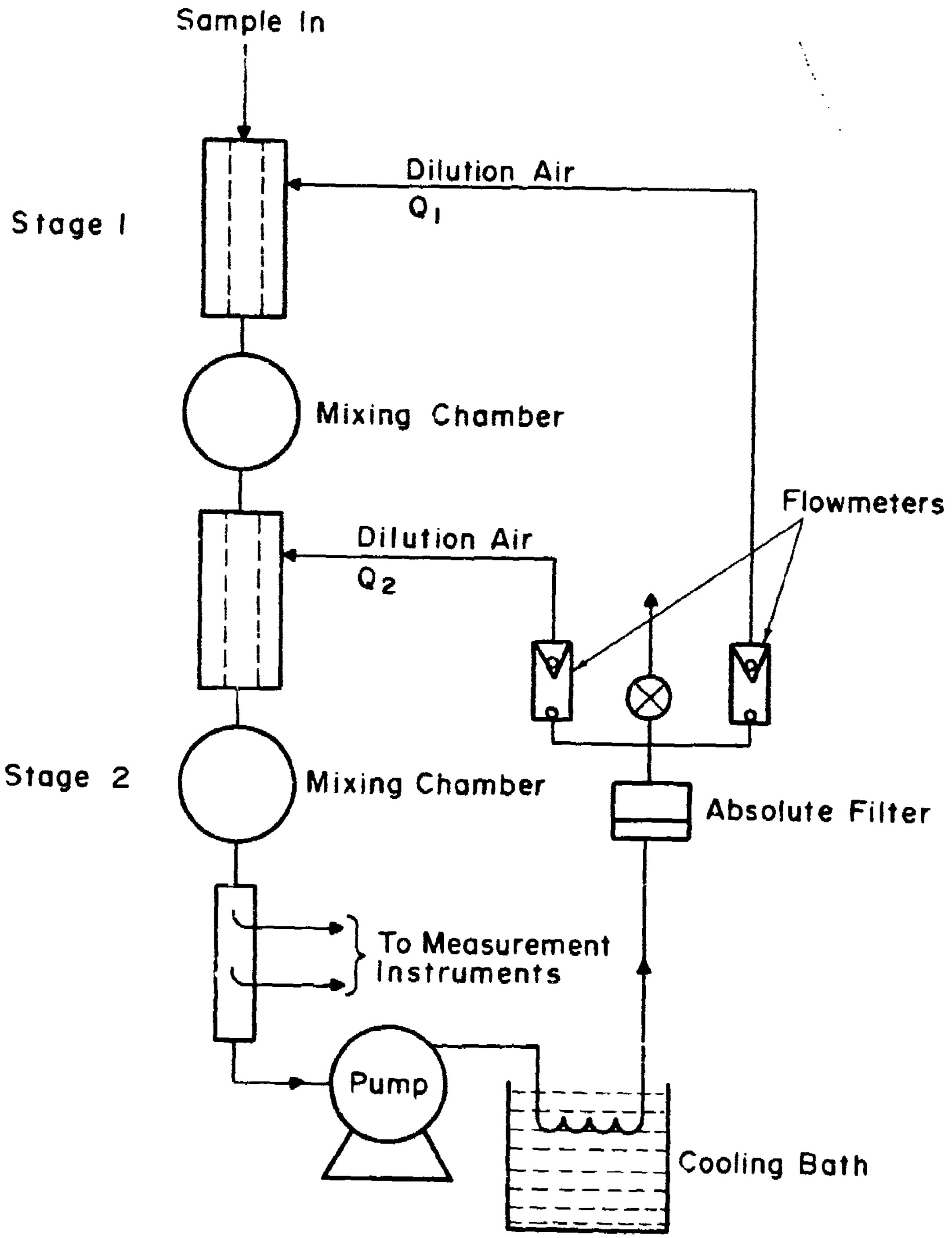

Figure 13. Aerosol sampling line and dilution system.

TABLE 15. PIEZOELECTRIC COUNTER STAGES

Stage	D_p50 µm	M_i µm
1	25.0	
2	12.5	18.75
3	6.4	9.6
4	3.2	4.8
5	1.6	2.4
6	0.80	1.20
7	0.40	0.60
8	0.20	0.30
9	0.10	0.15
10	0.05	0.075

After passing through the 10th, lowest, stage, the air flows through a flowmeter to a pump where it is exhausted to the atmosphere. The rate of frequency shift in each stage is related to the mass concentration of aerosol particles captured in that stage, and can be expressed by the following equation:

$$\frac{\Delta f_i}{\Delta t} = \sigma_i V C_i$$

where

Δf_i = frequency shift for stage i, Hz
Δt = sample time, min
σ_i = sensitivity factor for stage i
V = volume flow rate of air sample, 240 ml/min
C_i = aerosol mass concentration in stage i, µg/m³

The sensitivity factor, σ_i, depends on the resonant frequency of the crystal and the area of the sensitive portion of the crystal compared to the area of the impinging air jet, but is otherwise a constant for each stage. The concentration may therefore be calculated from the measured frequency shift by the equation:

$$C_i = k_i \frac{\Delta f_i}{\Delta t}$$

where

k_i = stage constant

The data reported from the P/Z cascade impactor are the total suspended particles (TSP) in mg/m^3 and the mass mean aerodynamic diameter, $\bar{d}m$, in µm. The TSP is determined by adding the masses per stage and multiplying by the dilution factor:

$$TSP = 1000\ \Sigma C_i$$

The $\bar{d}_m$ are computed by summing the products of the mass fractions per stage, X_i, times the midpoint cutoff size between stages, M_i:

$$\bar{d}m = \Sigma X_i M_i$$

where

$X_i = C_i/\Sigma C_i$

M_i = as indicated in Table 15

The Particle Measuring Systems, Inc. Active Scattering Aerosol Spectrometer (ASAS) Model ASAS-300-PMT was used for sizing particles within the size range of 0.088 to 3.00 µm. Particles passing through the laser cavity of a continuous He-Ne laser produce pulses of light proportional only to their size and position in the beam. A pair of photomultiplier detectors image the light impulses and select pulses produced by particles in the correct sample space. A pulse height analyzer then determines the particle sizes.

The ASAS output is the number distribution, $\bar{d}n$, of the suspended particles in µm. The mass median aerodynamic diameter, $\bar{d}m$ is obtained by multiplying $\bar{d}n$ by $\sqrt{\rho}$ where ρ is the particle density. The output of the ASAS is grouped into size classes as shown in Table 16.

TABLE 16. ASAS SIZE RANGE DATA

ASAS Range	ASAS Channel	Size Interval µm	Interval Width µm	d_i, Midrange Diameter, µm
3	1-7	0.088-0.144	0.056	0.116
3	8-15	0.144-0.208	0.064	0.176
2	4-15	0.210-0.390	0.180	0.300
1	4-8	0.388-0.503	0.115	0.445
1	9-15	0.508-0.676	0.168	0.592
0	2	0.690-0.855	0.165	0.772
0	3	0.855-1.020	0.165	0.938
0	4	1.020-1.185	0.165	1.102
-	-	-	-	-
0	15	2.835-3.000	0.165	2.918

A total of seven experiments was run with humidities ranging from 5% to 75%. Table 17 shows the list of experimental runs and the number designation for each run. The humidity during each experiment was monitored and Figure 14 shows the humidity inside the chamber as a function of time with the aerosol in it.

TABLE 17. LIST OF EXPERIMENTAL RUNS

Experiment Number	Weight of Munition gms.	RH %	Temp. °C
1	0.0726	24.5	24°F
2	0.1856	35	23°F
3	0.14	53	23°F
4	0.064	54	23°F
5	0.1856	53.5	24°F
6	0.185	75	26°F
7	0.1136	5	23°F

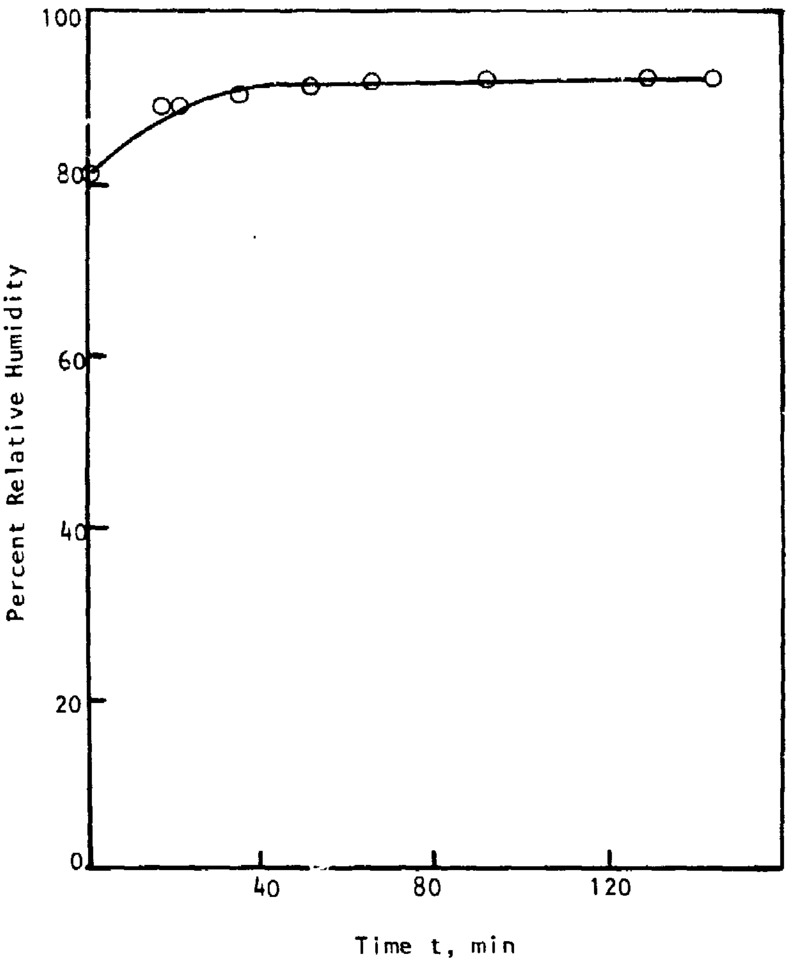

Figure 14. Percent relative humidity vs. time in aerosol chamber.

6.2 RESULTS AND DISCUSSION

A summary of the analysis of the data is given in Table 18. The mass mean diameters obtained from the measurements range from 0.4 μm to about 1.2 μm in the humidity range of 5% to 75%. The data obtained with the ASAS does not show any sensitivity to the humidity range but the P/Z cascade impactor data shows smaller mean diameters at lower humidities. The effect of humidity is enhanced when the number median diameters are compared instead of mass mean diameters. The number median diameter is low at both the low and high ends of the humidity range and peaks in the middle. This is possibly due to two factors:

(1) The smaller particles grow bigger by absorbing moisture. Hence, at a lower humidity such as 5% the particle size is smaller than at intermediate levels, for example at 40% relative humidity.

(2) A further increase in humidity will make the smaller particles which were outside the range of the instrument initially grow into the lower end of the particle size range thereby increasing the number of smaller sized particles. This results in a lowering of the number mean and median diameters. Table 19 shows the mass median and number median diameter. In order to pinpoint the effect of humidity on particle size more experiments are needed. At this point it suffices to say that at the humidity levels typical of ambient conditions the particles size is not affected by the humidity.

The mass mean aerodynamic diameter $\overline{d}_m$, calculated from light scattering measurements by the ASAS is consistently lower than the measured value by the P/Z cascade impactor.

The following assumptions involved in the transformation of number distribution to mass distribution may be the causes of the difference.

- the particles are assumed to be spherical
- the refractive index of the particles is assumed to be uniform
- all the particles are of uniform density. The coarseness in the cutpoints of the impactor stages also may contribute to error in mass mean diameter measurements
- a particle density, ρ, of 1.8 has been assumed

TABLE 18. SUMMARY OF INITIAL PARTICLE SIZE DISTRIBUTION

Number	Weight W of Phosphorus Burned (gm)	R.H. %	Time of Measurement min	Mass Mean Aerodynamic Diameter, $\overline{d}m$, µm P/Z	ASAS
1	0.726	24.5	2	1.22	0.75
2	0.1856	35	2	0.918	0.79
3	0.14	53	6	1.206	1.01
4	0.064	54	4	0.51	0.81
5	0.1856	53.5	16	1.23	1.13
6	0.185	75	4	0.89	1.00
7	0.1136	5	31	0.42	1.00

TABLE 19. PARTICLE SIZE DISTRIBUTION OF WHITE PHOSPHORUS-FELT MUNITION SMOKE

Number	Weight Of Munition Burned (gms)	R.H. %	P/Z			ASAS		
			MMD µm	σg	*R	NMD µm	σg	*R
1	0.0726	24.5	1.22	1.99	0.999	0.26	1.76	0.97
2	0.1856	35	0.904	1.96	0.995	0.179	1.76	0.987
3	0.14	53	0.793	2.12	0.987	0.198	2.15	0.91
4	0.064	54	0.408	2.54	0.997	0.25	1.63	0.991
5	0.1856	53.5	0.807	2.2	0.956	0.14	2.42	0.973
6	0.185	75	0.623	1.89	0.98	0.165	2.32	0.97
7	0.1136	5	0.308	1.77	0.98	0.138	2.41	0.98

*R = correlation coefficient

Figure 15 and 16 show typical histogram and cumulative log probabilities of the particle size distribution obtained in Experiment 3. Even though the data look bimodal in nature, a log normal distribution fits the data very well. This was true for all experiments. The fitting was done with all the data points weighted equally. To confirm whether the distribution of the data is bimodal or not requires more precise measurements with particle size monitors with finer intervals and broader operating ranges. Figure 17 shows the cumulative plot for Run No. 7, the 5% relative humidity run. The mass median diameter for this run is much smaller than for the other runs.

Time histories of mass mean diameter and TSP were obtained for Experiments 1 through 7. As an example, the complete data obtained up to two hours after the generation of smoke in Experiment 3 are given in Table 20. The decrease in mass concentration and the growth in particle mass mean diameter are plotted versus time in Figures 18, 19 and 20. The mean diameter increases and the mass concentration decreases linearly. Table 20 also gives the slope, m, intercept b, and correlation coefficient R for the equation

$$y = mt + b$$

where

$y = \bar{d}_m$ in μm
t = time

Table 20 is repeated in Appendix 1 with the corresponding data for Experiments 1-2 and 4-7.

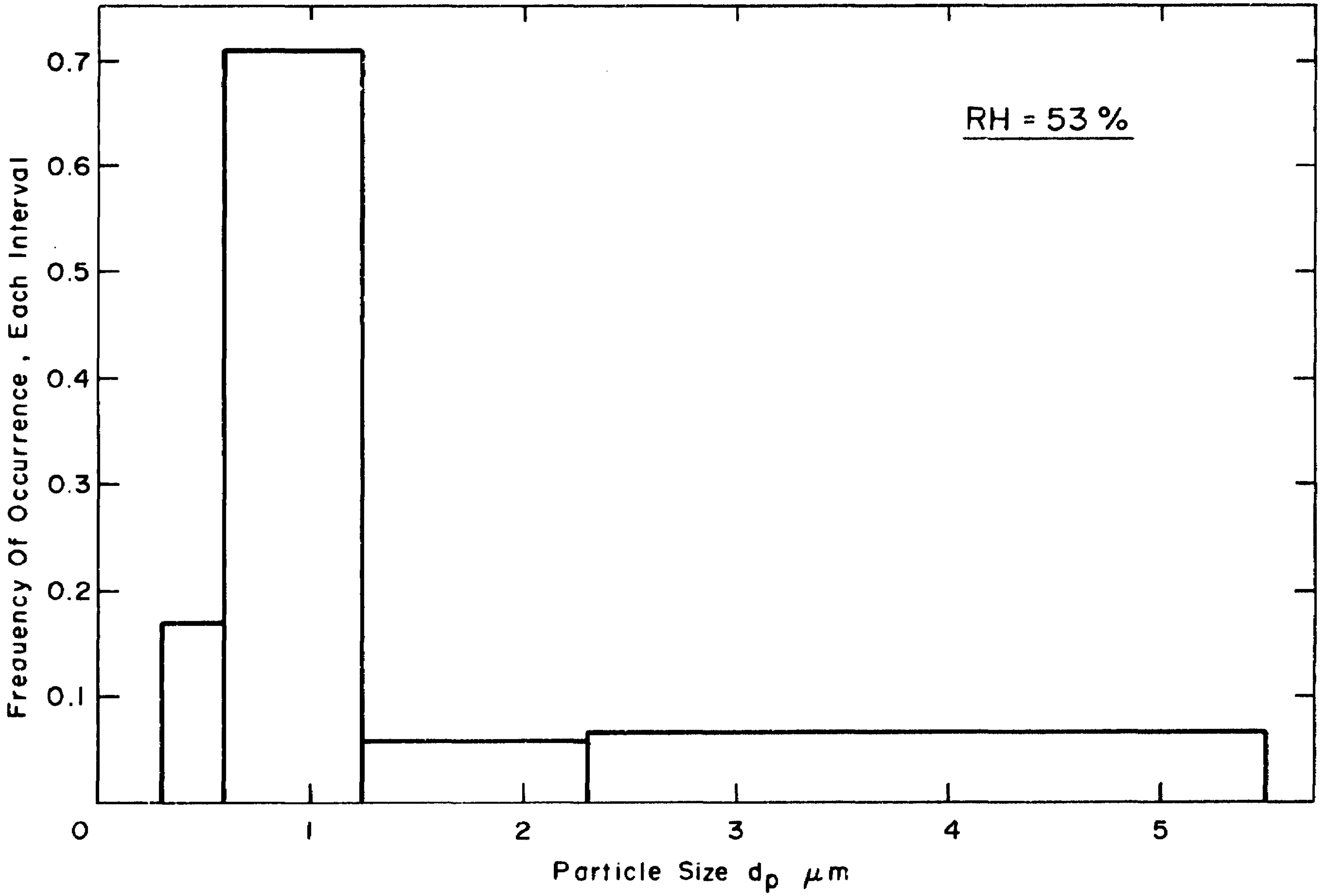

Figure 15. Experiment No. 3, histogram of frequency of occurence

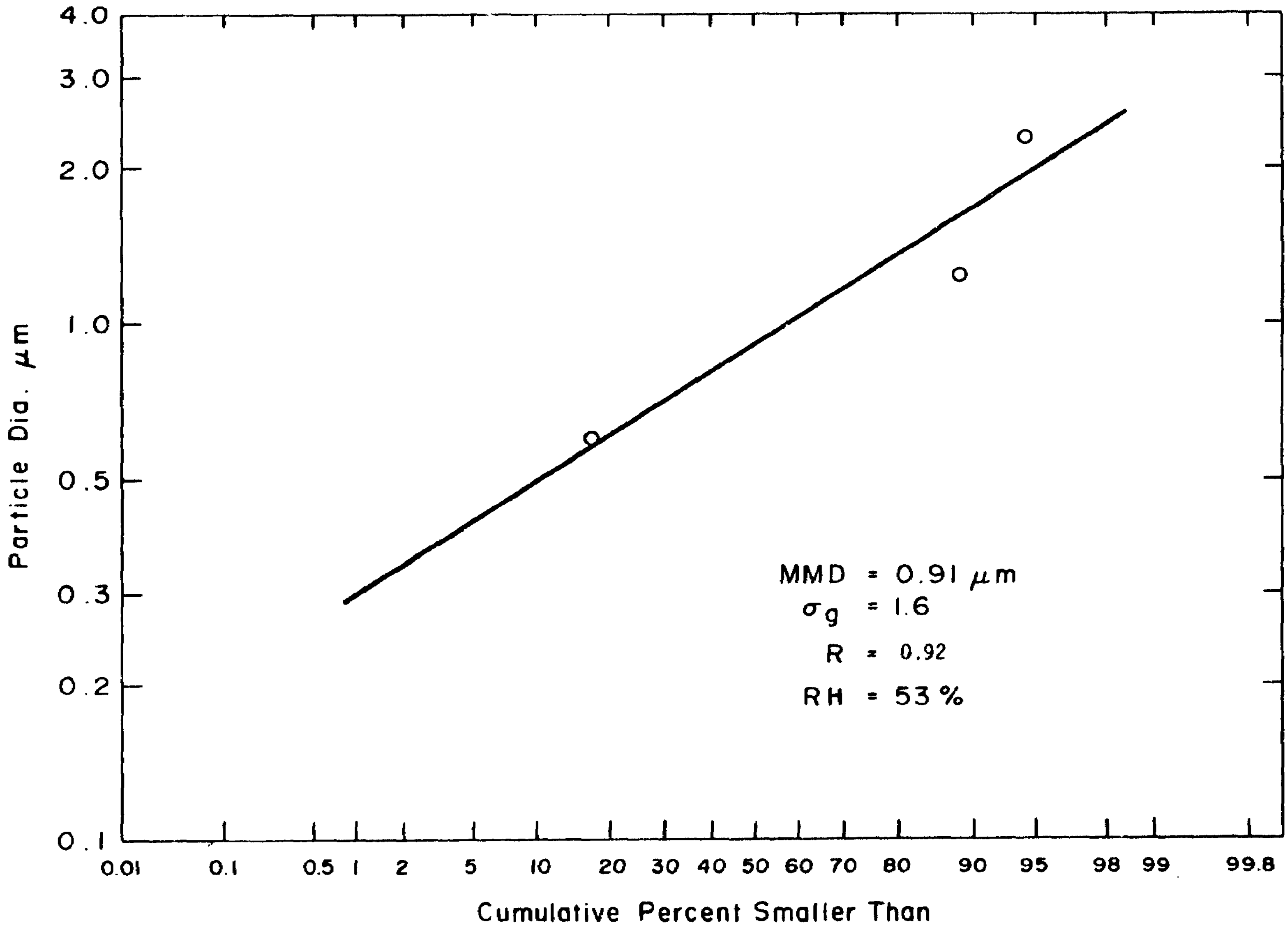

Figure 16. Experiment No. 3, particle size distribution

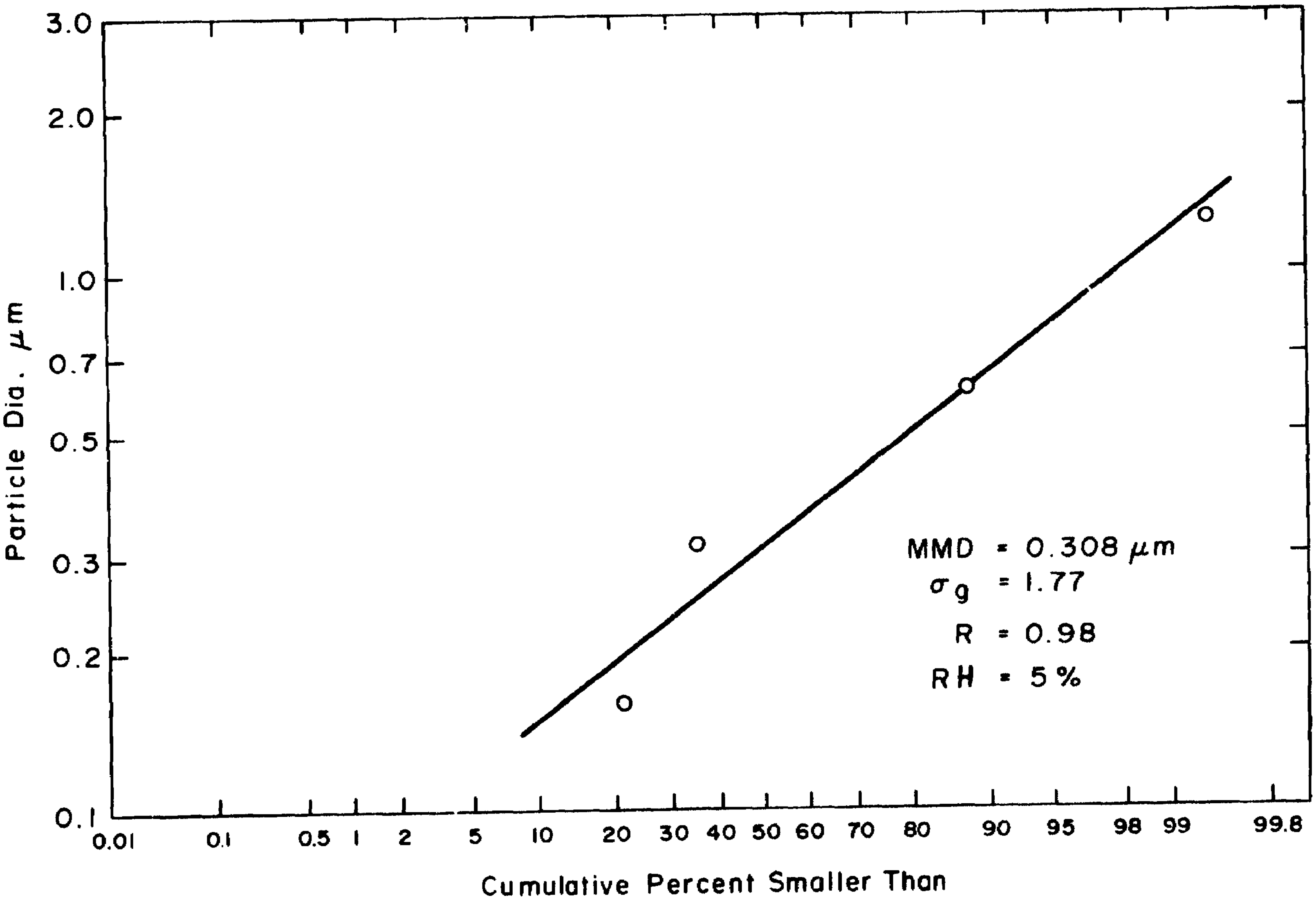

Figure 17. Experiment No. 7, particle size distribution

TABLE 20. TIME HISTORY FOR EXPERIMENT 3

53% Relative Humidity

P/Z Impactor			ASAS		
Time, min.	TSP $\mu g/m^3$	$\bar{d}m$, µm	Time, min.	Number of Particles, cm^{-3}	$\bar{d}n$, µm
6	93.90	1.206	4	586	0.78
15	156.76	1.114	6	1081	0.76
24	148.05	1.153	10	1740	0.77
41	213.20	1.169	14	2020	0.80
58	203.90	1.272	27	1349	0.90
77	204.20	1.229	31	1574	0.91
132	85.89	1.326	38	1596	0.87
			46	1074	0.92
			60	823	0.95
			74	662	0.95
			105	463	0.99
			130	314	1.03

$\bar{d}m = 0.0014t + 1.115$

R = 0.70

S.L. > 90%

$\bar{d}^3n = 0.0046t + 0.491$

R = 0.92

S.L. > 99%

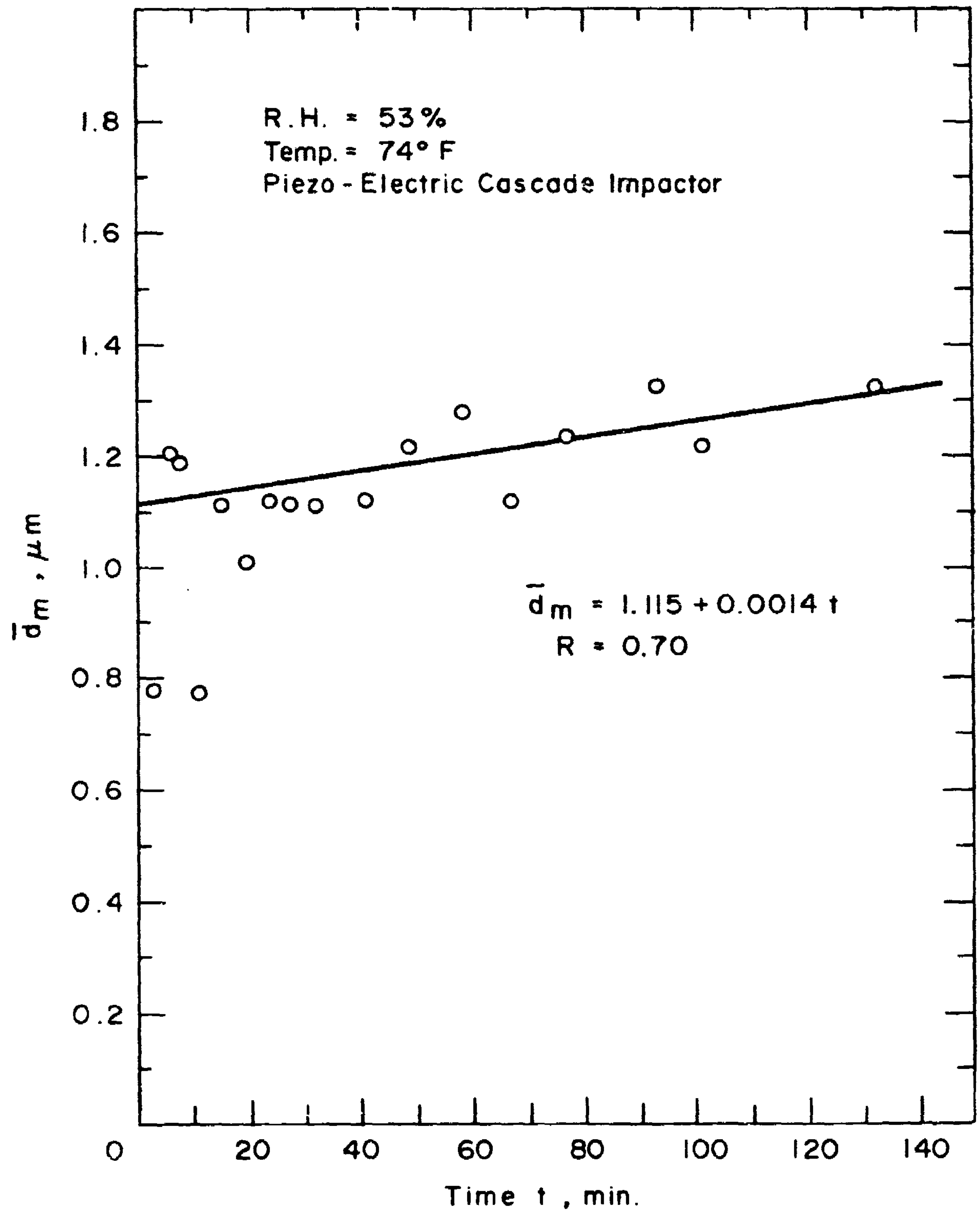

Figure 18. Experiment No. 3, growth of particle mass mean diameter vs. time

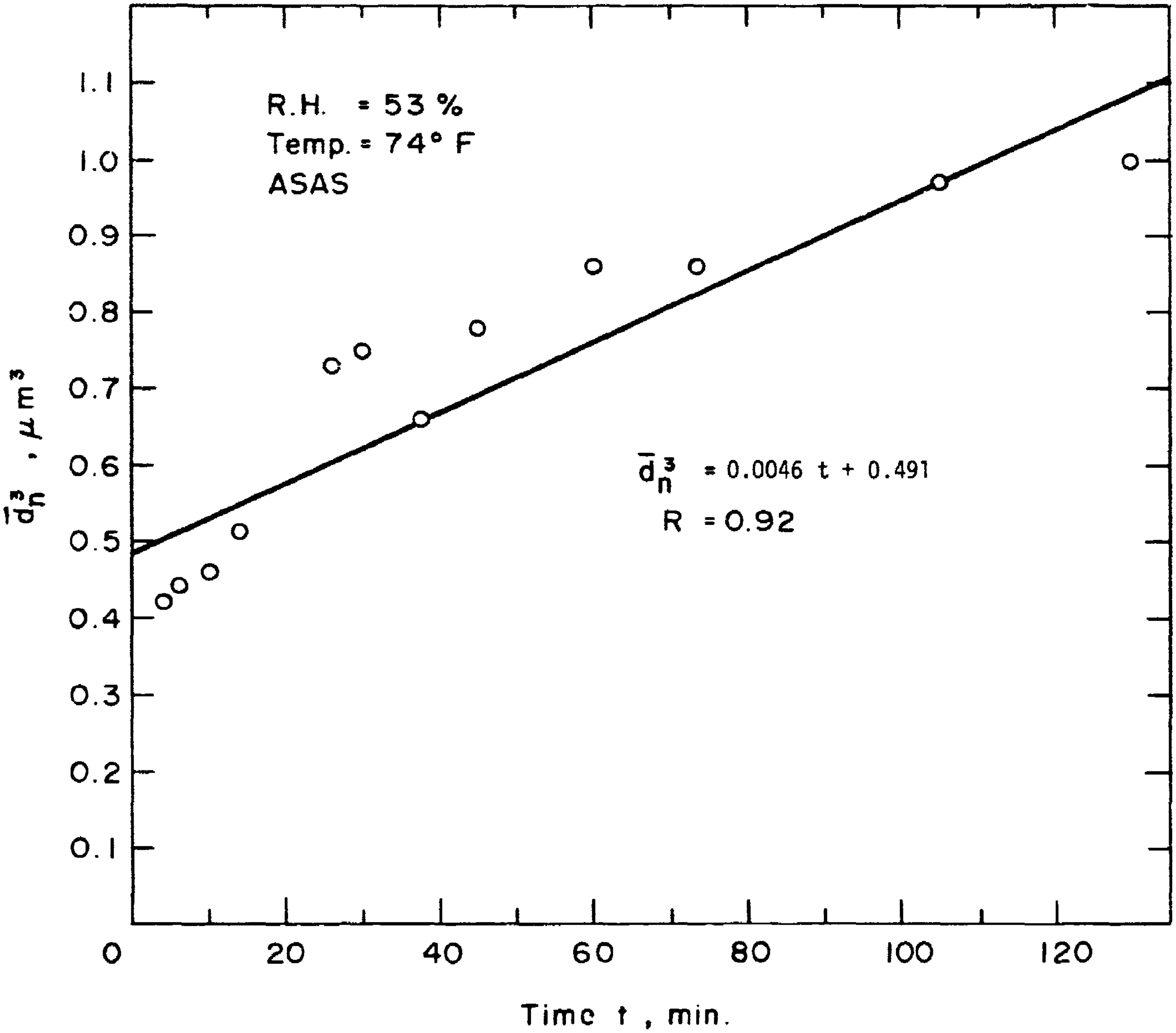

Figure 19. Experiment No. 3, growth of particle diameter vs. time

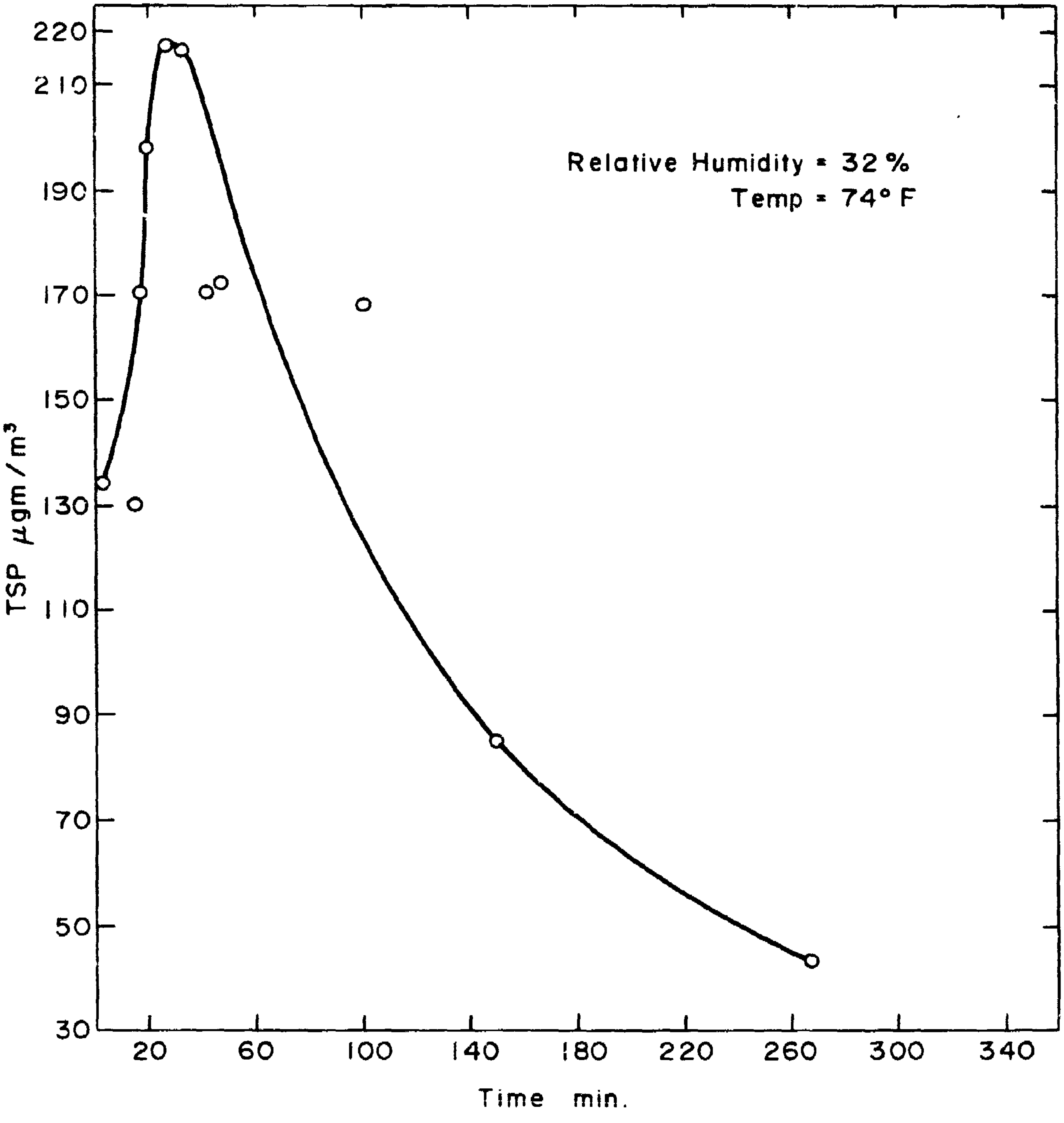

Figure 20. Experiment No. 3, aerosol mass concentration vs. time

APPENDIX

Aerosol Data for Experiments No. 1 to 7

The following Tables A-1 to A-7 list the experimental data on aerosol aging measured with the Piezoelectric Impactor and the ASAS Particle Spectrometer for Experiments No. 1 to 7.

The data include mean diameters and statistical correlations.

TABLE A-1. TIME HISTORY FOR EXPERIMENT 1

24.5% Relative Humidity

P/Z Impactor			ASAS		
Time, min.	TSP $\mu g/m^3$	$\bar{d}m$, μm	Time, min.	Number of Particles, cm^{-3}	$\bar{d}n$ μm
2	74.00	1.218	2	875	0.54
6	82.20	0.90	4	1084	0.55
14	121.20	1.212	6	1157	0.51
30	129.30	129.3	8	1256	0.64
45	159.00	159.0	10	1199	0.62
60	120.60	120.6	16	1256	0.67
			24	1090	0.62
			32	1156	0.68
			44	994	0.77
			61	657	0.72
			95	429	0.68
			151	367	0.87
$\bar{d}m = 0.0009t + 1.049$			$\bar{d}^3n = 0.0036t + 0.192$		
$R = 0.124$			$R = 0.93$		
S.L. < 90%			S.L. > 99%		

TABLE A-2. TIME HISTORY FOR EXPERIMENT 2

35% Relative Humidity

P/Z Impactor			ASAS		
Time, min.	TSP $\mu g/m^3$	$\bar{d}m$, µm	Time, min.	Number of Particles, cm^{-3}	$\bar{d}n$, µm
2	134.40	0.918	2	2316	0.55
17	147.60	1.180	4	2362	0.55
26	218.30	0.950	8	3153	0.59
45	172.80	1.280	14	3645	0.65
150	74.20		20	2637	0.69
			33	1111	0.81
			44	703	0.86
			55	854	0.84
			62	1165	0.90
			97	443	0.95
			150	277	0.97
			257	148	0.93
$\bar{d}m = 0.0018t + 0.98$			$\bar{d}^3n = 0.0055t + 0.245$		
$R = 0.72$			$R = 0.926$		
S.L. = 90%			S.L. > 99%		

TABLE A-3. TIME HISTORY FOR EXPERIMENT 3

53% Relative Humidity

P/Z Impactor			ASAS		
Time, min.	TSP $\mu g/m^3$	$\bar{d}m$, µm	Time, min.	Number of Particles, cm^{-3}	$\bar{d}n$, µm
6	93.90	1.206	4	586	0.78
15	156.76	1.114	6	1081	0.76
24	148.05	1.153	10	1740	0.77
41	213.20	1.169	14	2020	0.80
58	203.90	1.272	27	1349	0.90
77	204.20	1.229	31	1574	0.91
132	85.89	1.326	38	1596	0.87
			46	1074	0.92
			60	823	0.95
			74	662	0.95
			105	463	0.99
			130	314	1.03

$\bar{d}m = 0.0014t + 1.115$
R = 0.70
S.L. > 90%

$\bar{d}^3n = 0.0046t + 0.491$
R = 0.92
S.L. > 99%

TABLE A-4. TIME HISTORY FOR EXPERIMENT 4

54% Relative Humidity

P/Z Impactor			ASAS		
Time, min.	TSP $\mu g/m^3$	$\bar{d}_m$, µm	Time, min.	Number of Particles, cm^{-3}	$\bar{d}_n$, µm
4	75.20	0.51	2.5	495	0.60
10	67.00	0.96	4.5	531	0.55
20	55.00	0.92	10.5	568	0.60
40	80.00	1.16	16.5	578	0.62
50	55.20	1.17	24.5	530	0.59
61	61.40	1.23	28.5	486	0.63
			45.0	355	0.63
			52.5	321	0.66
			56.0	374	0.65
			62.0	316	0.66
$\bar{d}_m = 0.01t + 0.678$			$\bar{d}^3_n = 0.0015t + 0.192$		
$R = 0.87$			$R = 0.88$		
S.L. = 95%			S.L. > 99%		

TABLE A-5. TIME HISTORY FOR EXPERIMENT 5

53% Relative Humidity

P/Z Impactor			ASAS		
Time, min.	TSP $\mu g/m^3$	$\bar{d}m$, μm	Time, min.	Number of Particles, cm^{-3}	$\bar{d}n$, μm
16	196.80	1.23	13	1866	0.84
27	197.60	1.36	15	1919	0.85
50	148.00	1.43	19	2209	0.91
62	160.00	1.16	25	1939	0.89
95	110.80	1.16	31	3017	0.92
156	86.00	0.98	41	905	0.93
			60	742	1.07
			97	510	1.06
			157	316	1.01
			240	256	1.02

$dm = -0.002t + 1.377$

$R = -0.77$

S.L. = 90

$\bar{d}^3n = 0.0077t + 0.54$

$R = 0.91$

S.L. > 99

TABLE A-6. TIME HISTORY FOR EXPERIMENT 6

75% Relative Humidity

P/Z Impactor			ASAS		
Time, min.	TSP µg/m^3	$\bar{d}m$, µm	Time, min.	Number of Particles, cm^{-3}	$\bar{d}n$, µm
4	371.6	0.889	2	6821	0.764
12	408.0	0.860	4	6101	0.767
22	379.6	0.886	6	6085	0.809
44	329.2	0.977	8	5854	0.778
65	223.6	1.580	14	5543	0.789
88	199.6	1.686	22	5006	0.844
120	172.4	1.200	30	4523	0.842
			46	4263	0.887
			60	3364	0.861
			70	2901	0.896
			99	2090	0.936
			120	1367	0.927

$\bar{d}m = 0.0056t + 0.868$	$\bar{d}^3n = 0.003t + 0.478$
R = 0.69	R = 0.94
S.L. = 90%	S.L. > 99%

TABLE A-7. TIME HISTORY FOR EXPERIMENT 7

5% Relative Humidity

P/Z Impactor			ASAS		
Time, min.	TSP $\mu g/m^3$	$\bar{d}m$, µm	Time, min.	Number of Particles, cm^{-3}	$\bar{d}n$, µm
31	7993.5	0.416	2	7335	0.750
44	6812.0	0.455	4	6914	0.72
63	4532.0	0.383	8	6785	0.72
82	2946.0	0.396	14	5897	0.77
			20	5606	0.76
			31	2359	0.78
			41	2922	0.78
			52	2411	0.82
			65	1745	0.84
			86	1072	0.86

$\bar{d}m = -0.0008t + 0.456$

$R = -0.587$

S.L. < 90%

$\bar{d}^3n = 0.003t + 0.383$

$R = 0.96$

S.L. > 99%

REFERENCES

1. H. Yamaguchi, T. Nakamura, Y. Hirai, and S. Ohashi, Journal of Chromatography, 172 (1979) 131-140.

PUBLICATIONS AND PERSONNEL

The following reports have been issued under Contract DAMD17-78-C-8085:

1. Physical and Chemical characterization of Fog Oil Smoke and Hexachloroethane Smoke. Part I, Final report on Hexachloroethane Smoke January 1980.
2. Physical and Chemical Characterization of Military Smokes. Part II, White Phosphorus Felt Smokes. May 1981.
3. Physical and Chemical Characterization of Military Smokes. Part III, White Phosphorus Felt Smokes. May 1981.

The following personnel participated as follows:

Part I	Part II	Part III
R. Farlow	R. Butler	W. Bock
S. Katz	R. Farlow	R. Butler
S. Mainer	S. Katz	S. Katz
A. Snelson	S. Mainer	N. Rajendran
R. Welker	N. Rajendran	S. Relwani
	A. Snelson	A. Snelson
	R. Welker	

DISTRIBUTION LIST

25 copies	Commander US Army Medical Bioengineering Research and Development Laboratory Attn: SGRD-UBC Fort Detrick Frederick, MD 21701
4 copies	USAMRDC (SGRD-RMS) Fort Detrick Frederick, MD 21701
12 copies	Defense Technical Information Center (DTIC) Attn: DTIC-DDA Comeron Station Alexandra, VA 22314
1 copy	Dean School Of Medicine Uniformed Services University of the Health Sciences 4301 Jones Bridge Road Bethesda, MD 20014
1 copy	Commandant Academy of Health Sciences, US Army Attn: AHS-CDM Fort Sam Houston, TX 78234
1 copy	Commander US Army Medical Bioengineering Research and Development Laboratory Attn: SGRD-UBD-A/Librarian Fort Detrick Frederick, MD 21701